Reconstructing Fault History from Fault Rocks and Travertine, Rock Canyon Fault, Utah

Senior Thesis

Submitted in partial fulfillment of the requirements for the

Bachelor of Science Degree

At The Ohio State University

By

Joel C. Main

The Ohio State University

2011

Approved by

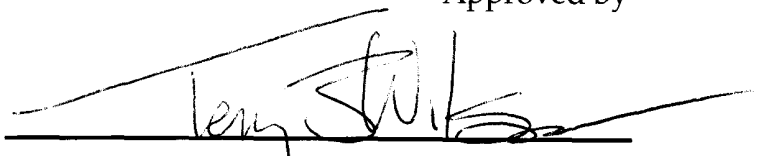

Terry J. Wilson, Advisor
School of Earth Sciences

Abstract

In the Basin and Range Province (BRP) in central Utah a horst and graben structure is oriented perpendicular to the BRP's N-S trending horst and graben blocks. The northern fault (Rock Canyon Fault) of this anomalously oriented structure and its related faults rocks are being studied to better understand how it has evolved through time and its relation to the BRP deformation. The evolution of Rock Canyon Fault is shown through its rocks, travertine and breccias, and their structures. Two brecciation processes have formed the rocks observed: fault void fill and explosive breccias. The structures in the rocks reveal a minimum of four alternating precipitation and brecciation events. Mapping the Rock Canyon fault zone shows a lateral distribution of the composition and thickness of the fault rocks. As Rock Canyon Fault progresses toward the Valley Fault (a BRP fault) it thickens and changes from calcite to primarily travertine. The Rock Canyon Fault and Valley Fault (main fluid flow conduit) is therefore thought to meet or intersect. To better understand how this fault has evolved through time and whether it is contributing to the BRP deformation stable isotope data needs to be collected on the Valley Fault and Rock Canyon Fault to reveal absolute age.

Acknowledgements

I would like to give special thanks my thesis advisor, Dr. Terry Wilson, for the opportunity to work on an amazing project with some of the coolest rocks I have ever seen. Her guidance, support, patience and time have helped mold me into a better geologist. Finally, I would like acknowledge her impressive mentor and advising skills, without them I would have been utterly lost.

My parents deserve more thanks than I can give. If it were not for their support, emotionally and financially, I would not be where I am today. They have been supporting throughout my whole life and I credit the majority of my successes to them.

A thanks to my officemates and friends Cristina Millan, Stephanie Konfal, Jamey Stutz, Bill Magee, Zack Trunkely, and Dave Saddler. I am going to miss relying on such a supporting, open, and funny group. Wish the best to you all and hope to keep in touch.

To the faculty and staff at the Department of Earth Sciences for their support, teaching, knowledge, and genuine interest in student success. Also, to geology friends I have met throughout the years. I can safely say that you guys are my best friends.

Lastly, I want to thank the financial sponsors of my project: OSU's Undergraduate Research Office, Friends of Orton Hall (FOH), Geological Society of America (GSA), and American Geophysical Union (AGU). I would not have been able to further my research or attend professional geology conferences if it were not for these grants and scholarships.

TABLE OF CONTENTS

1. Introduction

Travertine is a calcium carbonate ($CaCO_3$) rock that forms when supersaturated carbon dioxide (CO_2) fluid reservoirs within the Earth seep through cracks or faults and crystallize $CaCO_3$ out of solution (Brogi et al., 2010; Brogi and Capezzuoli, 2009; Faccenna et al., 2008; Hancock et al., 1999; Pentecost, 2005; Wright et al., 2009; Zentmyer et al., 2008). The geometry and textures of travertine deposits associated with faults provide a record of the flux of CO_2-rich fluids along the fault through time (Brogi and Capezzuoli, 2009; Cakir, 1999; Faccenna et al., 2008), and of fault history and seismicity associated with faults (Brogi et al., 2010; Mesci et al., 2008; Minissale et al., 2002; Shipton et al., 2004; Uysal et al., 2007; Uysal et al., 2011). Fault rocks, such as breccias and associated veins also provide a record of faulting events and the evolution of fault behavior. Breccias and travertine deposits along faults can provide information about the location of potentially hazardous faults, about the history of earthquakes along faults, on fault motions, and on the interactions between circulating hydrothermal fluids and fault geometry and activity. Studying stable isotopes in travertine layers can reveal paleoclimate during the successive slip and fluid flow events (Brogi and Capezzuoli, 2009; Brogi et al., 2010; Faccenna et al., 2008; Minissale et al., 2002; Uysal et al., 2009; Uysal et al., 2011; Zentmyer et al., 2008). Modern examples of CO_2 leakage along faults are being studied as natural analogues for processes associated with carbon sequestration (Dockrill and Shipton, 2010; Shipton et al. 2004). These studies can help answer questions such as what controls the migration of CO_2, and if CO_2 is sequestered in a CO_2 reservoir in Earth's subsurface, will it remain trapped there?

During mapping for The Ohio State University (OSU) Field Geology course in central Utah, travertine deposits and breccias were discovered along the east-west trending Rock Canyon fault (Wilson, pers. comm., 2010). The objectives of this study are to document the

evidence of fault history contained in travertine and breccia formed along the Rock Canyon fault in order to test whether this is a young, potentially active structure contributing to Basin and Range Province deformation.

1.1 Geological Setting

The Basin and Range Province in the Western United States is a region of the continent that is actively stretching due to motion on an array of normal faults that form regional, north-south trending mountain blocks and valleys. Central Utah lies along the eastern border of the Basin and Range Province, where normal faulting is superimposed on the Sevier fold and thrust belt (Figure 1). Within this region, the Sanpete Valley is a major extensional basin, bounded by the Valley Fault against the uplifted San Pitch Mountains (Gunnison Plateau) horst block to the west (Figure 2a). Along the San Pitch Mountains the north-south Valley normal fault (Fong, 1995) is intersected by a graben structure between Rock Canyon and Dry Canyon with an anomalous east-west orientation relative to other Basin and Range structures (Figure 2b). The northern fault zone bounding this east-west graben is called here the Rock Canyon fault zone, and is the focus of this study.

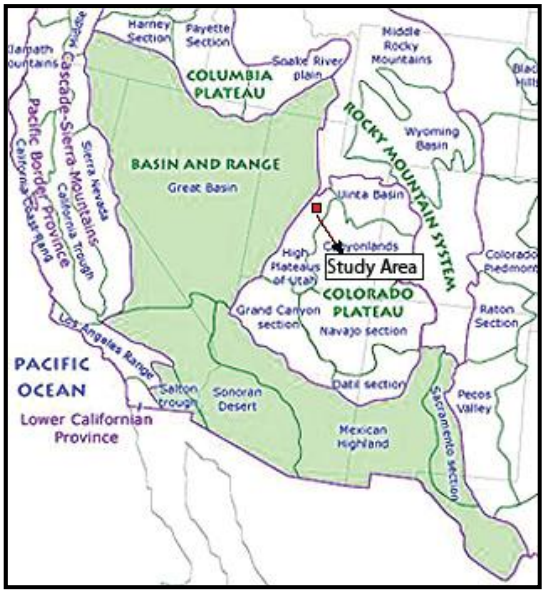

Fig. I *Study area in relation to the Basin and Range Province.*

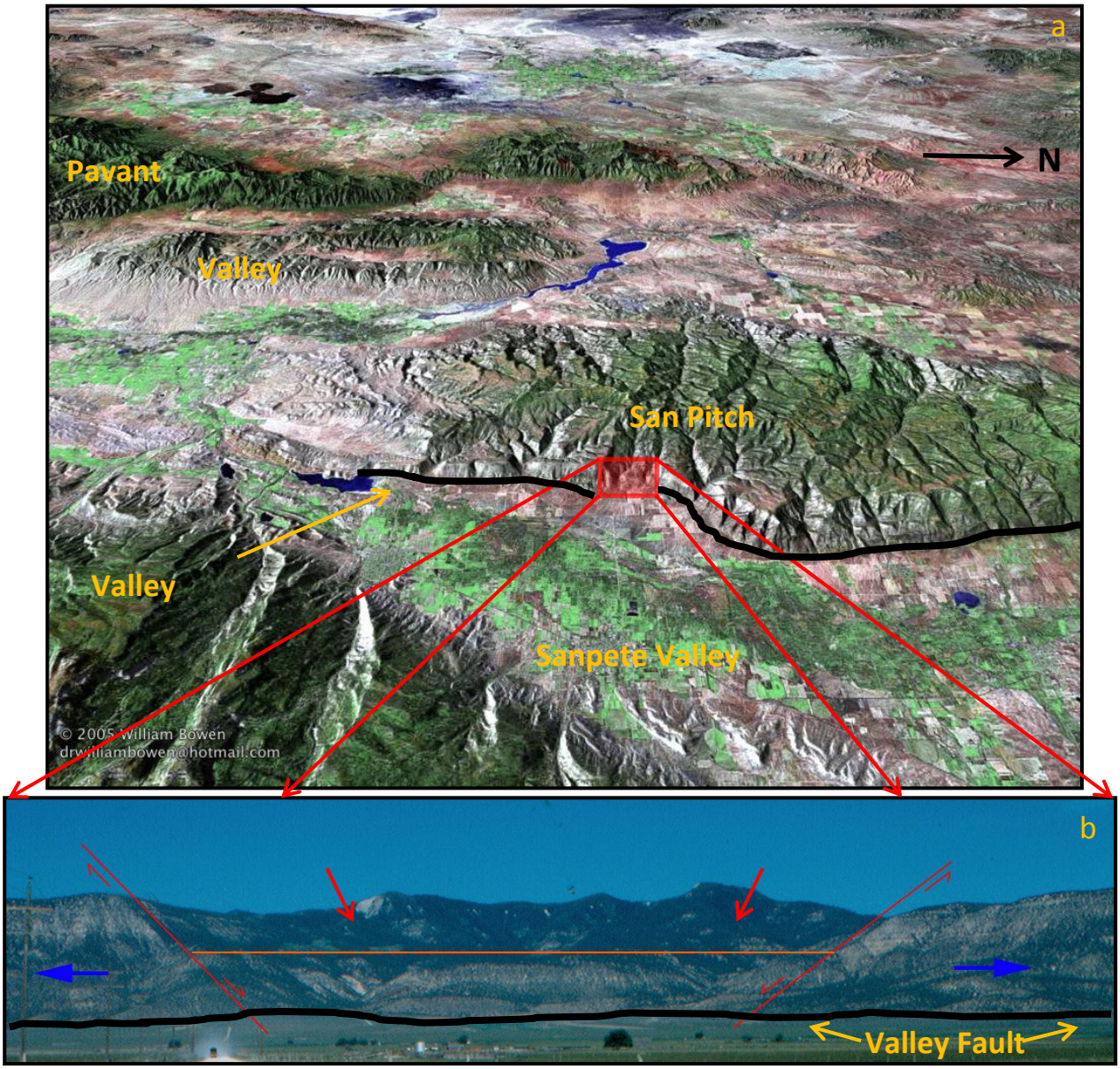

Fig. 2 a) *Aerial photograph of Eastern Basin and Range Province. The black line is the listric Valley Fault along the eastern boarder of the San Pitch Mountains. The red square encompasses Rock and Dry Canyons.* b) *View to the west across the Sanpete Valley of the horst and graben in Rock and Dry Canyons. Red lines represent normal faults, the orange line is the top of the graben, the black line is the Valley Fault, and the blue arrows represent the extension direction that caused the structure seen in area.*

2. Methodology

2.1 Mapping

During OSU field camp 2010, reconnaissance mapping and sampling along the most prominent fault in the Rock Canyon fault zone was completed by Wilson (pers. communication, 2010). The following year more detailed mapping of faults within the Rock Canyon fault zone was completed for this study. The distribution of fault breccias, calcite veins and travertine deposits along the fault traces were mapped. Three relatively well-exposed areas, including one large zone of calcite and two large zones of travertine, were mapped in detail. Oriented (*in situ*) and non-oriented samples were collected for laboratory observation. Structural data were collected on planar and linear features along each fault by measuring the attitudes of calcite and travertine veins, fault planes and striae. Each field site where samples and structural data were collected was recorded as a GPS 'waypoint' taken with a portable Garmin GPS 12 XL.

The fault zone map and detailed maps were scanned and digitized using Adobe Illustrator CS4 and ArcGIS10 software packages. The field fault map was georeferenced and the faults were traced on topographic maps, geologic maps and aerial photography using ArcGIS 10. The attitude of the main Rock Canyon fault was determined from the map using the three point problem. GPS waypoints were imported into ArcGIS so that types of breccia, thickness of travertine, and presence of calcite and/or travertine at each locality could be plotted laterally along each fault zone. The field data was organized into an Excel spreadsheet according to location with descriptive notes.

2.2 Direct Rock Observations

Systematic observations of fault rocks and fault-associated veins were made at three different scales – outcrop, hand sample and microscopic. To compare and integrate these observations field photos, digital scans and associated notes were compiled for each location in a portfolio. Outcrop characteristics of fault rocks and vein deposits were recorded in photos, notebook sketches and detailed maps.

Hand samples were washed and slabs were cut perpendicular to the fault zone margins and to travertine laminae to show any orientations and/or symmetry relative to fault planes. Three dimensional sketches were drawn of the sample to track each cut made to the rock and to preserve known *in situ* orientation of samples. Slabs were polished to improve visibility of textures and were scanned and edited in Adobe Photoshop. Digital and paper sketch maps were made of textures and structural features in the rock slabs.

Slabs were cut into billets and sent to Spectrum Petrographics, Inc. for thin sectioning. Thin section structures in the travertine were observed using a petrographic microscope. Compositional differences in the travertine laminations were studied using a cathodoluminescence (CL) microscope. The CL microscope consists of a vacuum chamber and electron beam. A sample, slab or thin section, is placed in the chamber that is then sealed and vacuumed. The electron beam is absorbed by the molecules in the sample increasing the energy level of the atoms (cathodoluminescent centers) causing them to glow before they transfer the energy through inelastic collisions and return to their ground state (Barker and Wood, 1986). CL shows geochemical information within the sample that provides important information on composition, texture and structure (McLemore and Barker, 1987). CL can reveal different

sources of fluids that the precipitate formed from and the growth rings of a mineral (McLemore and Barker, 1987). The samples observed under the CL microscope did not show luminescence though not all potential samples were observed.

2.3 Structural Analysis

Structural measurements collected in the field were compiled for each mapped fault and categorized based on structure type in an Excel spreadsheet. The data were entered into the Stereonet software package (freeware from R. Allmendinger, http://homepage.mac.com/nfcd/work/programs.html). Each type of planar structure was assigned a unique color and then plotted as great circle traces on stereoplots for each fault. Contours of poles to planes were plotted using contour interval of five percent per 1% area to determine the average attitude of each structure type. Linear structures were plotted as points, and also contoured to determine average attitude.

3. Results

3.1 Mapping

In the summer of 2011 I mapped the eastern portion of the Rock Canyon fault zone. The same area was mapped by Lawton and Weiss (1999), who found four south-dipping normal faults in the fault zone; the longest of the four faults being the southernmost fault (Figure 3). My mapping shows that the fault zone consists of four high-angle, south-dipping faults and one high-angle, north-dipping fault (Figure 4). These faults are labeled A-F, with "A" being the southernmost fault and "F" being the northernmost fault in the Rock Canyon fault zone. Fault A is the most prominent fault, being the most laterally continuous at ~1070 meters, very well

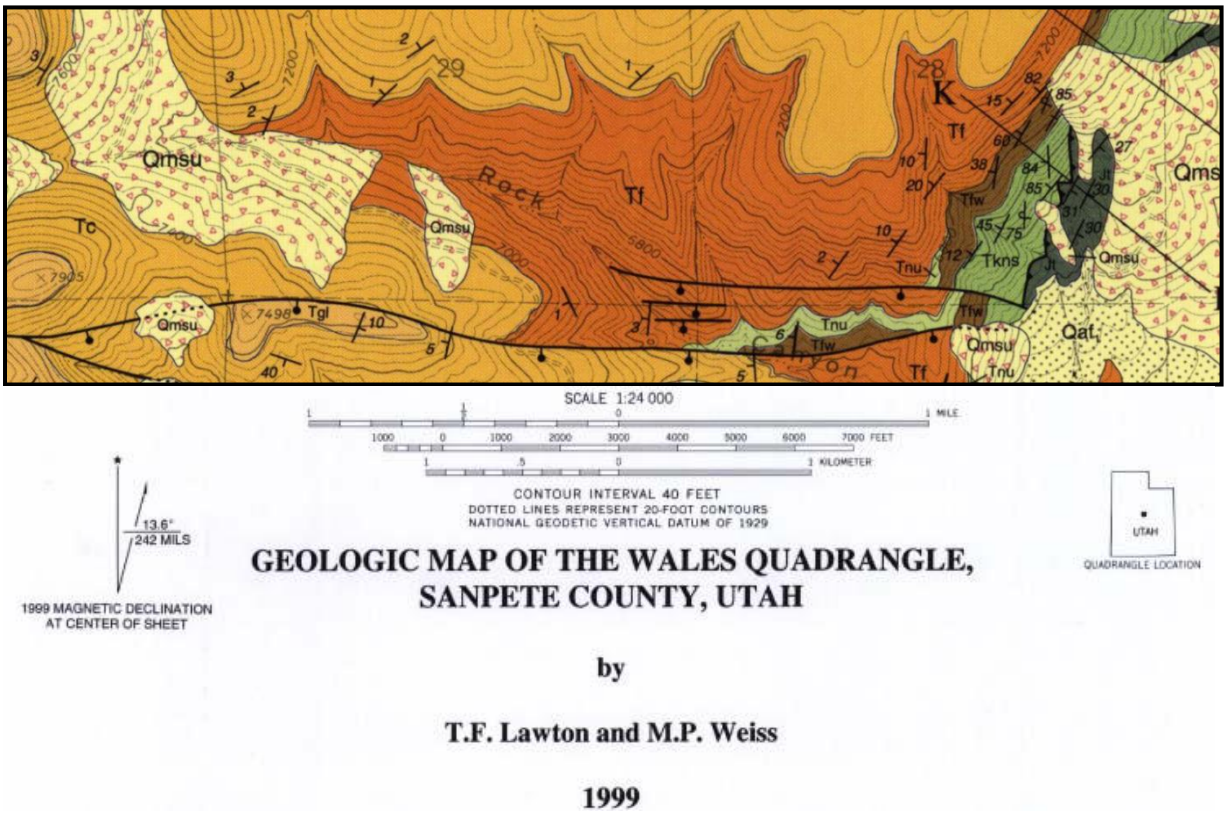

Fig. 3 *Geologic map from the Wales Quadrangle by T.F. Lawson and M.P. Weiss (1999) displaying four normal faults in the Rock Canyon fault Zone. Unit symbols used in the geologic map include: Jt, Jurassic Twist Gultch Formation: TKns, Cretacious-Tertiary (Paleogene) North Horn Formation; Tnu, Upper red bed member of the North Horn Formation; Tfw, Wales Tongue of the Flagstaff Limestone; Tf, Tertiary (Paleogene) Flagstaff Limestone; Tc, Tertiary (Paleogene) Colton Formation; Tgl, Lower member of the Green River Formation, Qaf, Quaternary alluvium fan deposits; Qmsu, Quaternary slide and slump deposits.*

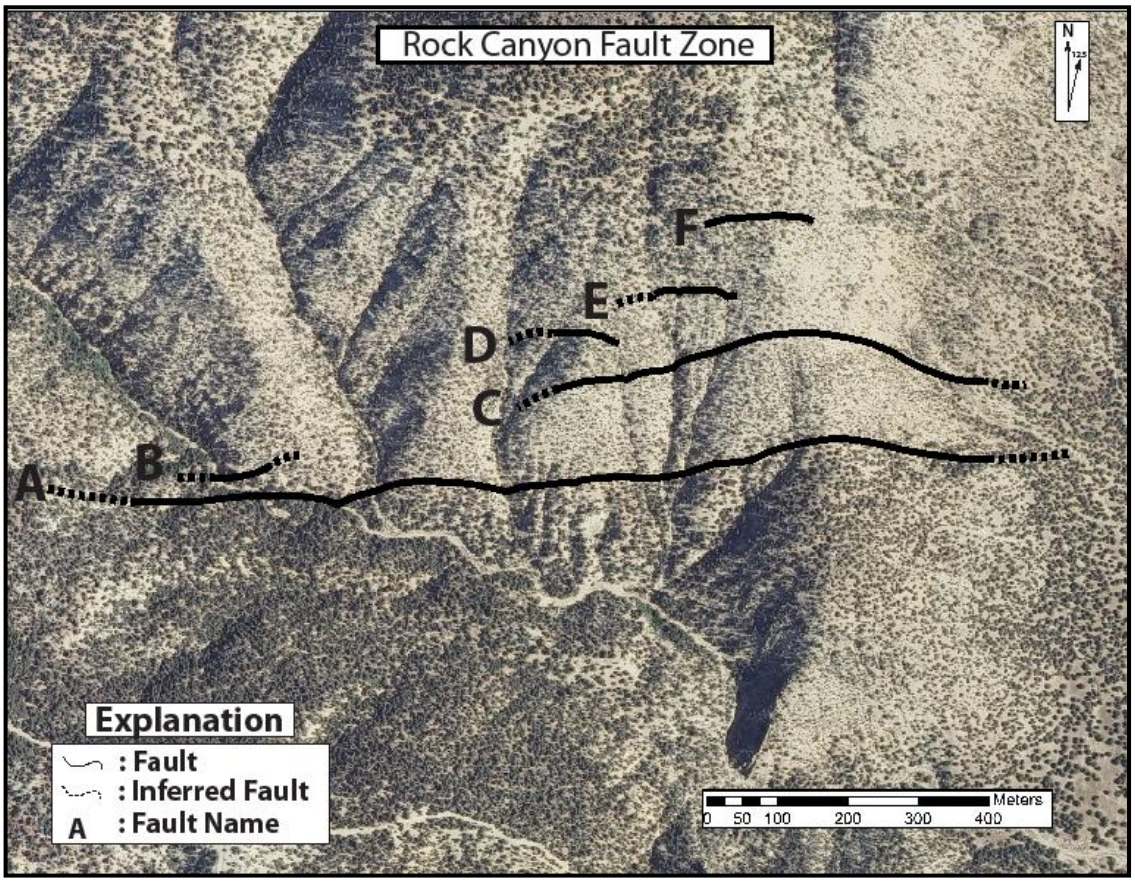

Fig. 4 *Georeferenced aerial photograph (http://mapserv.utah.gov/rasterindicies/naip2009.html) of Rock Canyon fault zone with Fault A (Rock Canyon Fault) mapped in 2010 and Faults B-F mapped in 2011.*

exposed, and with the largest offset, followed by Fault C. The Colton (Pgc), Flagstaff (Pgf), and North Horn (PgKn) formations are cut and displaced by Fault A. The zone displays a normal dip separation of stratigraphic contacts. Constructing a cross section and using the hanging wall and footwall cutoffs of the contact between Pgc and Pgf with Fault A, I found a total stratigraphic dip separation of 260 meters for the fault zone. Fault C cuts Pgf and PgKn and has exposed outcrop for ~650 meters. Fault B cuts only PgKn, cannot be followed laterally, and has a dip to the north. Slickenfiber steps on Fault C document hanging wall-down, normal slip. Faults E and F cut only Pgf, cannot be followed laterally, have dips to the south, and display fault-plane slickenfibers. The slickenfiber steps on Fault E show left lateral movement. The slickenfiber steps on Fault F display right-lateral movement.

The attitude of Fault A was determined by the 3-point problem (Rowland et al., 2007). On the contour map, where the fault crosses the same contour twice, a line is drawn. This line represents the strike of the fault and is measured to be N83E. The dip is determined by the equation (tan δ = change in elevation/map distance). For Fault A tan δ = (520/180) = 2.88. So δ = $\tan^{-1}(2.33)$ = 70.96 or ~71 degrees south. The attitude of Fault A is N83E, 71S.

Figure 5 is a detailed map of a section of Fault A. In this section three approximately tabular, parallel calcite veins from 1 cm to 15 cm in thickness (Figure 6a) are present along the fault in the North Horn formation. A breccia containing calcite and siltstone clasts is exposed along with the southeast margin of the fault exposure at this locality (Figure 6b). Growth direction was determined by observing calcite crystal characteristics (explained in a later section). Each vein in this map represents a separate episode of opening-mode fracture, fluid flow, and calcite precipitation (e.g. [1], [2], and [3] in Figure 5). The breccia represents a slip

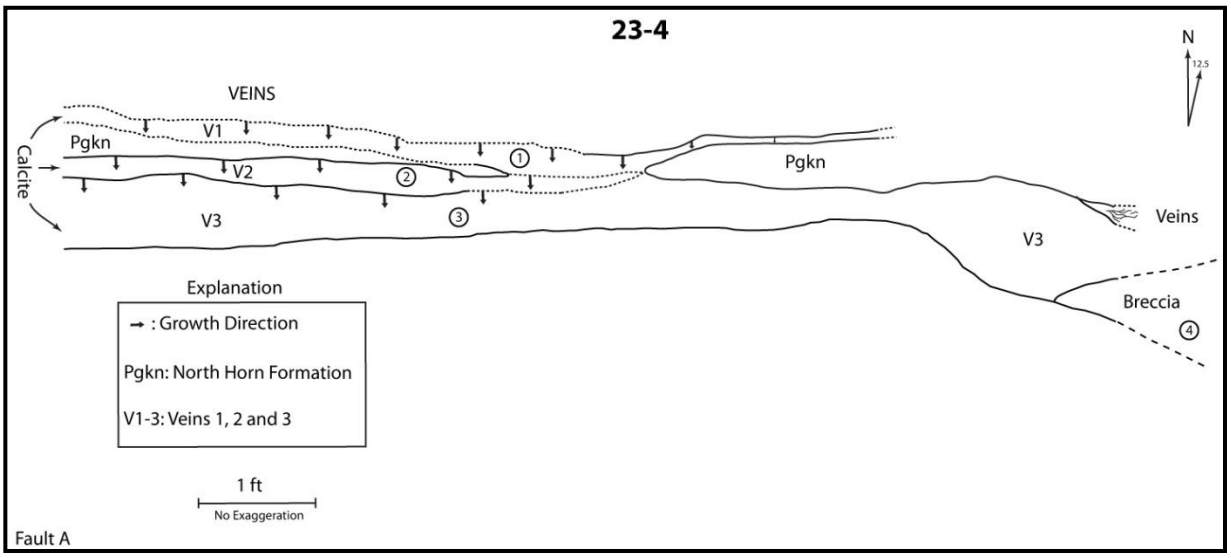

Fig. 5 *Detailed map of Fault A showing three calcite veins and crystal growth directions along with a breccia in the southeast corner.*

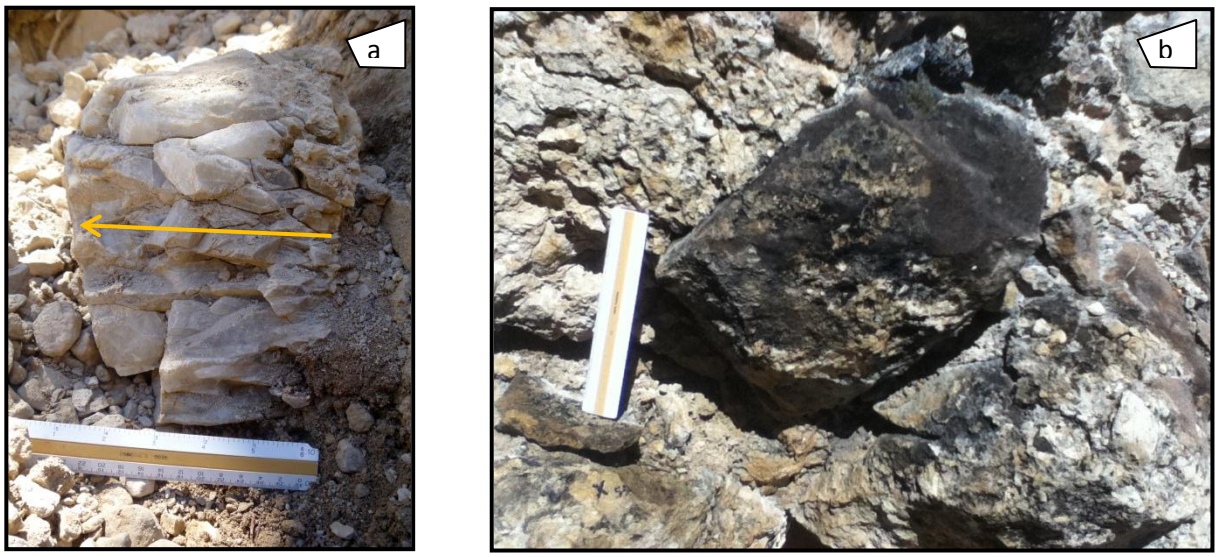

Fig. 6 *a) Calcite vein (V3) from map 23-4 with growth direction indicated. b) Breccia with clasts of siltstone and sandstone from the North Horn formation from Figure 8 (map 25-1).*

event along Fault A. This map documents three separate fracture/fluid pulse events and one slip/brecciation event.

Figure 7 shows a section of Fault C. This section contains fault-parallel veins consisting of zones of elongate calcite crystals, a zone of laminated travertine and a breccia zone. Veins with elongate calcite are present along the northern and southern margins of the E-W trending fault. Crystal growth directions are indicated with arrows on the travertine and calcite. The laminated travertine zone is 0.6 meter wide, forming a band parallel to the fault. A 0.55 meter wide zone of breccia forms the northern part of the fault zone. Three phases of fluid flow have occurred precipitating both calcites and the travertine. The travertine laminations represent

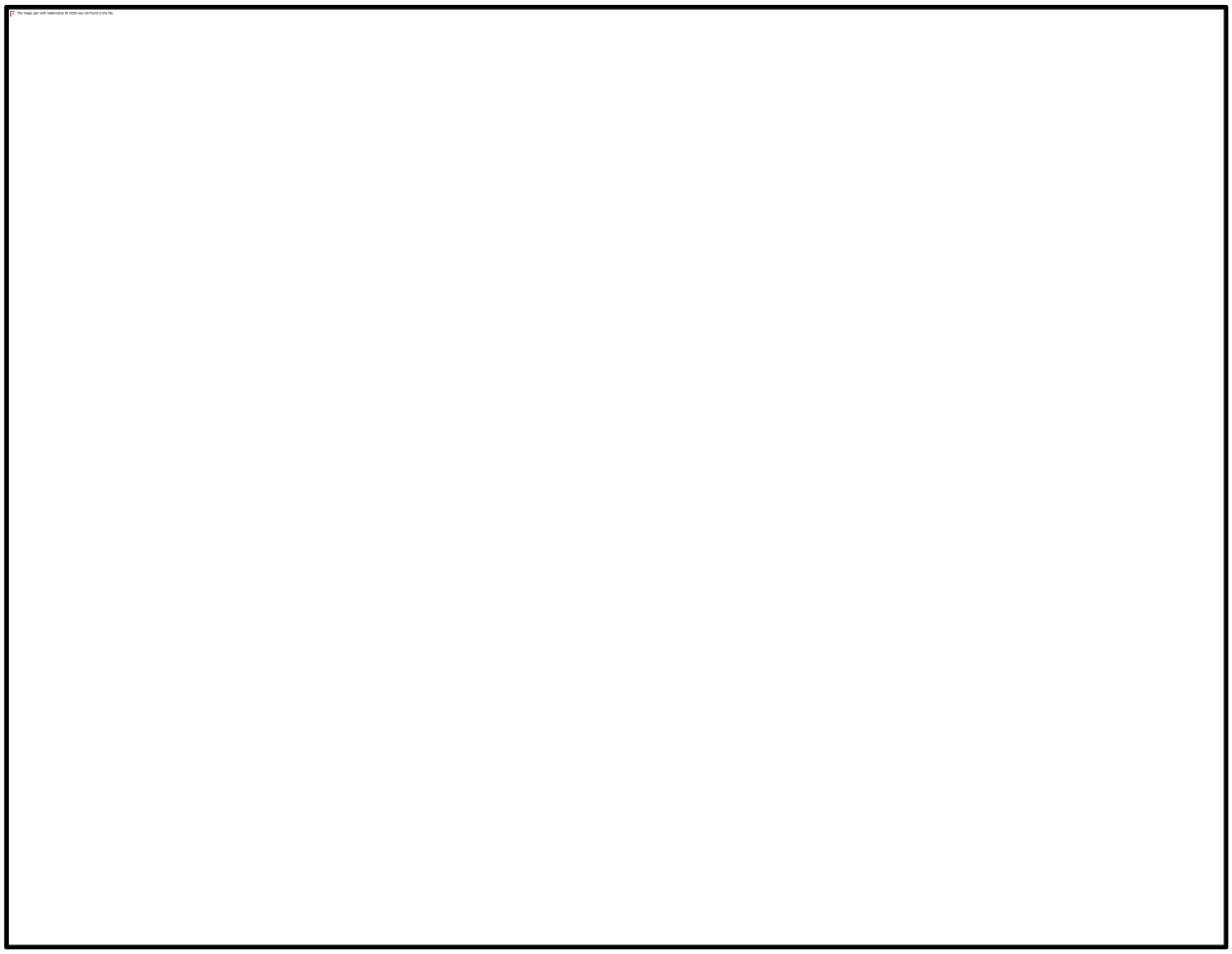

Fig. 7 *Detailed map of Fault C showing precipitation of both calcite and travertine with breccia composed of travertine and calcite cement.*

pulses of fluid flow or variations in fluid composition and temperature (Pentecost, 2005). Stable isotopic data is required to discriminate the factors controlling the development of lamination. The presence of the breccia records a minimum of one faulting event.

Figure 8 is a detailed map of the 19.3 meter thick travertine and breccia zone at the eastern end of Fault A. This region exhibits large quantities of brecciated travertine with clasts of travertine, sandstone and siltstone. Clasts range from 1 cm to 20 cm in diameter (Figure 6b) and in some cases are fully rimmed by travertine laminae (Figure 9). The middle region of the fault

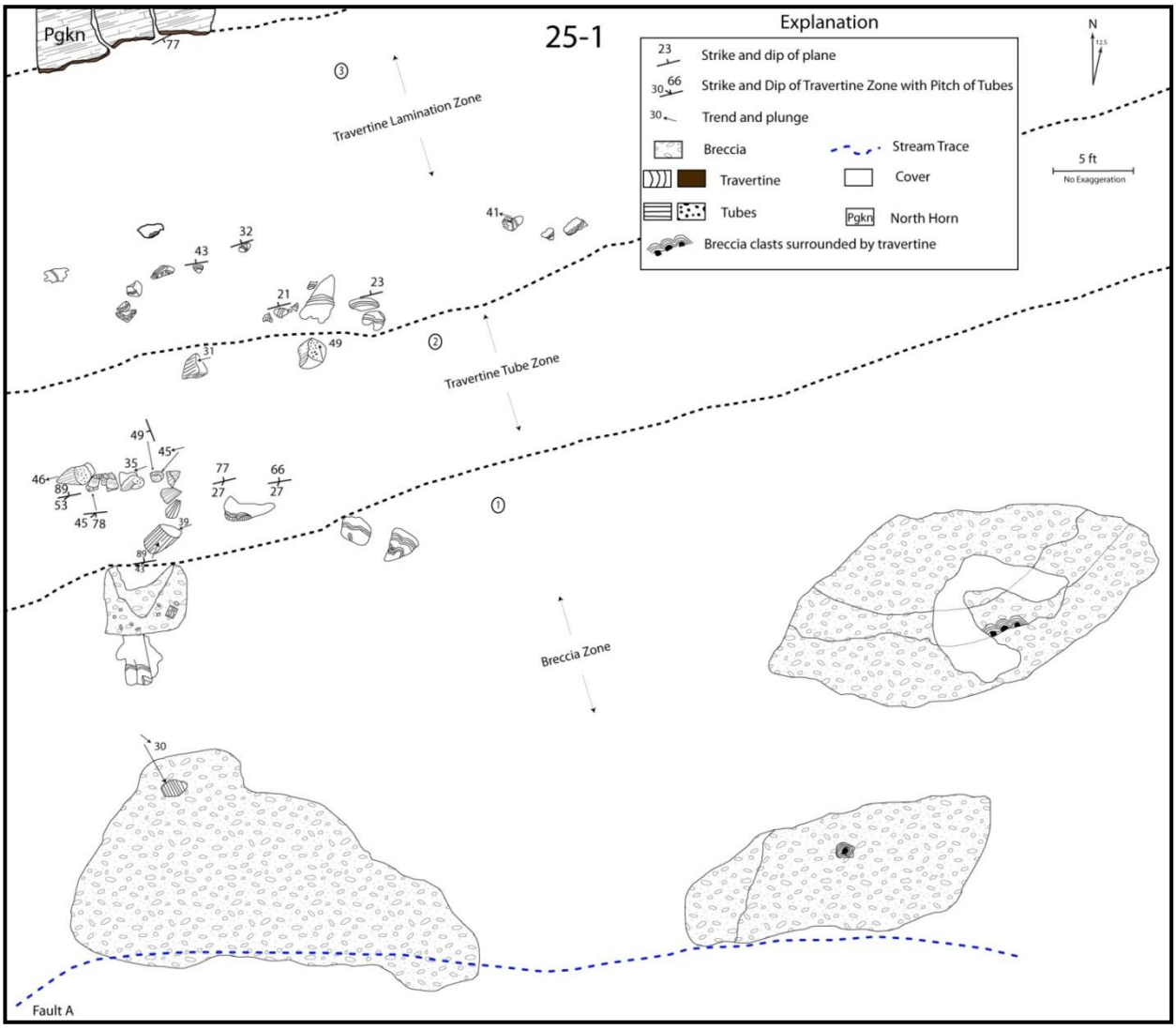

Fig. 8 *Detailed map of Fault A showing two different travertine morphology zones followed by a breccia zone in the south.*

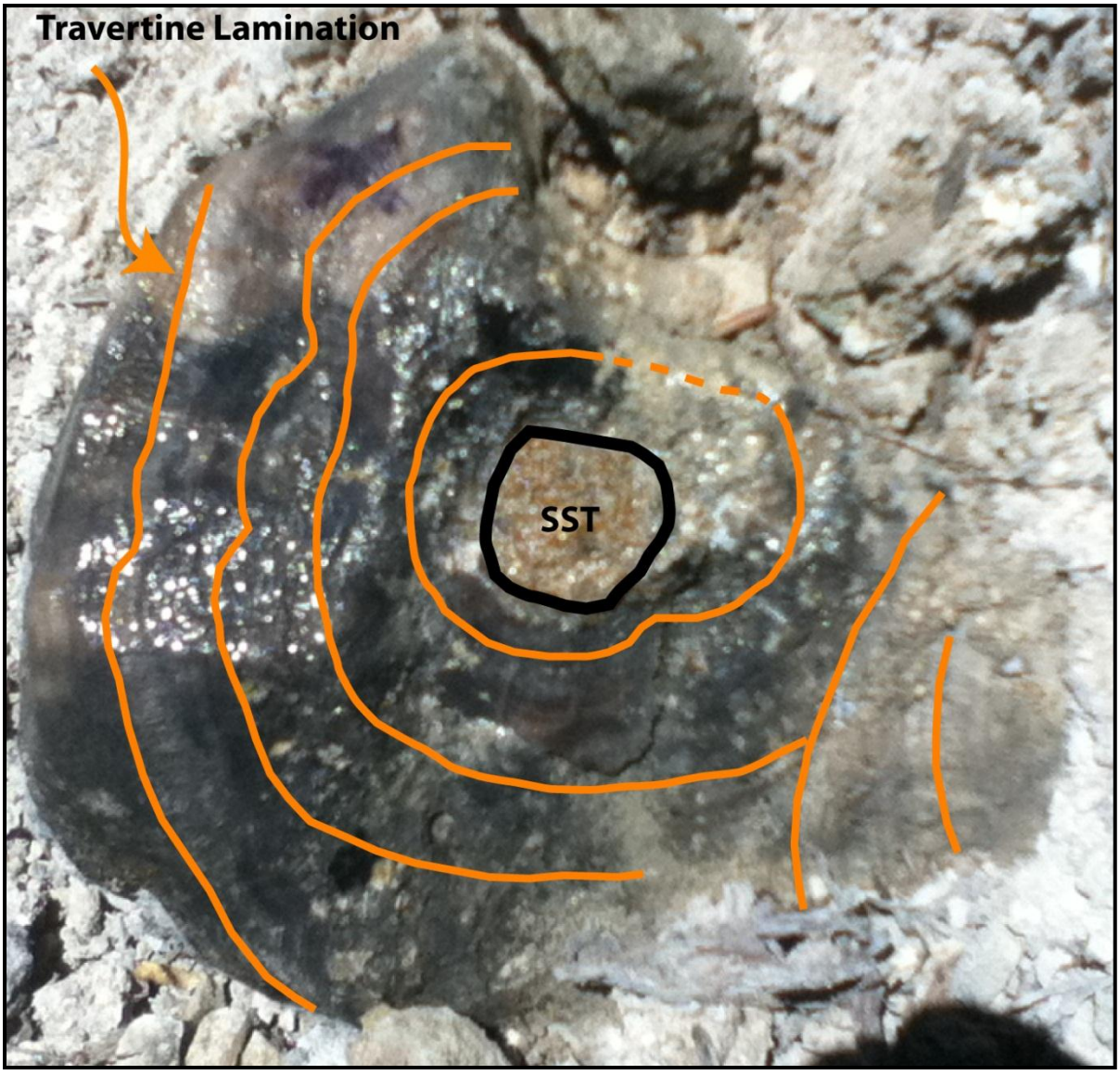

Fig. 9 *Picture of a sandstone clast fully surrounded by laminated travertine. From map 25-1 (illustrated in the southeastern breccia).*

zone contains pink-tan tubular travertine. The long axes of these travertine tubes have an oblique orientation to the walls of the fault zone. A zone of laminated travertine forms the northern portion of the fault zone, adjacent to the North Horn formation. This map reveals a minimum of one brecciation event and a minimum of two precipitation events. Again, factors controlling the lamination development cannot be discriminated without isotopic data.

3.1.1 Distribution of Vein Types and Fault Rocks

Mapping along the Rock Canyon fault zone demonstrates lateral variation in the type and thickness of both fault breccias and vein deposits (Figure 10). Thickness (t) is defined here as the width of the fault zone perpendicular to fault margins, including internal zones of calcite and travertine veins and of breccias. The westernmost part of Fault A examined in this study consists of zones of calcite and/or breccia less than one meter thick. Eastward, the zone widens to 1 meter $\leq t < 10$ meters. The easternmost sector widens to $t \geq 10$ meters, with the easternmost exposure having t = 19.33 meters. The difference in zone thickness from west to east is 19.33m - .002m = 19.31 meters in a distance of 1070 meters.

Laterally, there is a close relationship between zone thickness and composition. The western region of the fault zone displays only calcite in veins up to 2 cm wide. Moving eastward, the central region of the fault zone has both calcite and travertine veins. The eastern region contains primarily travertine. From west to east the zone progressively widens and changes in composition from calcite, to calcite and travertine, to primarily travertine.

In Figure 11 the types of breccias are mapped on Fault A and C and consist of both chaotic and crackle breccias. Three localities of crackle breccia exist in the central region: two on Fault A and one on Fault C. The dominant fault rock along all of the faults is chaotic breccia, which

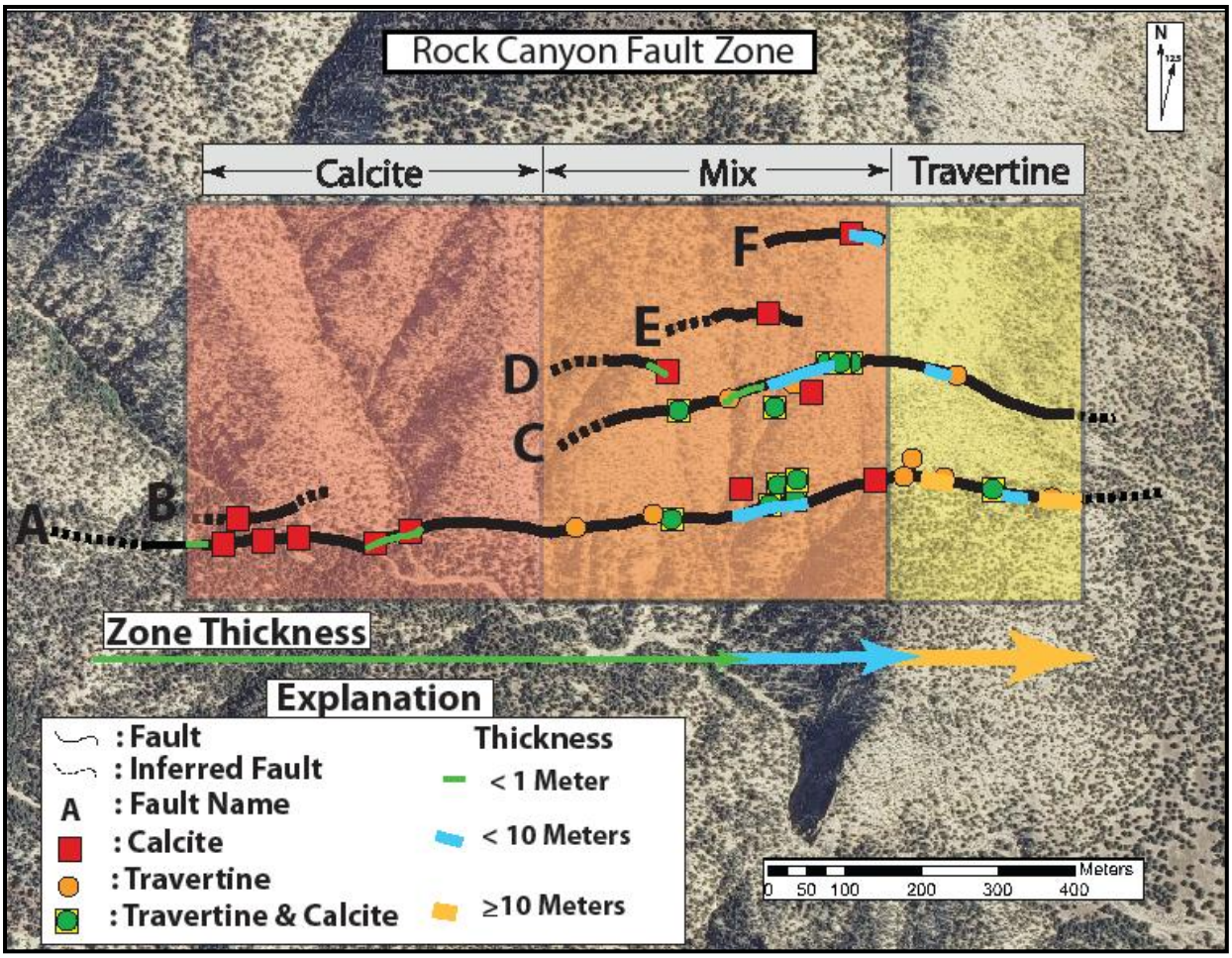

Fig. 10 *Map of rock types along Faults A-F, thickness of individual fault zone (calcite, travertine, breccia, and host rock in between) and dominant rock type laterally across the fault overlain on an aerial photograph of Rock Canyon.*

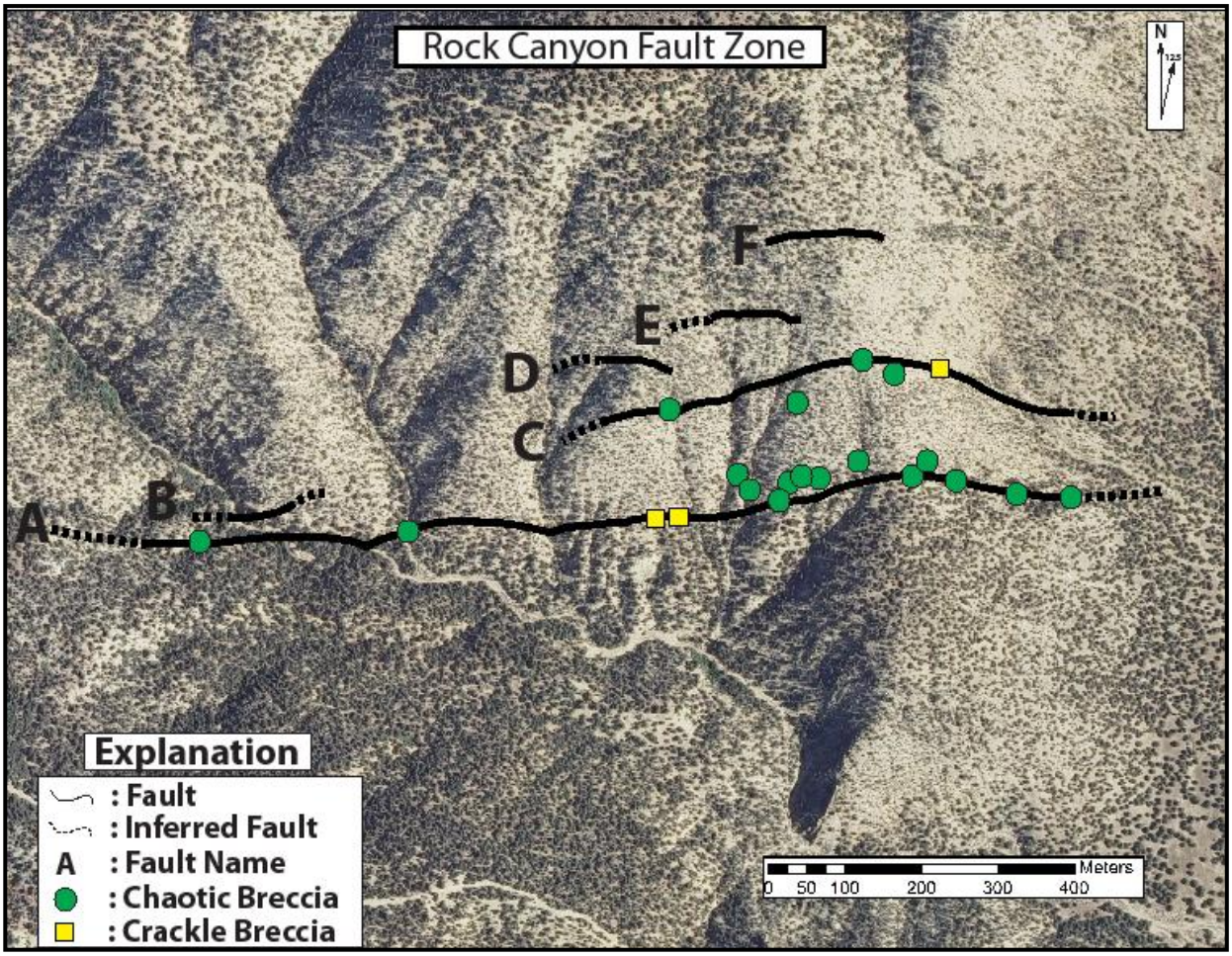

Fig. 11 *Map of breccia type along Faults A and C*

occurs along the whole fault zone.

3.2 Travertine

The travertine bodies in the study area were found in steeply dipping veins and, most commonly, in veins parallel to the fault margins. Travertine laminae form parallel to the growth surface (Shipton et al., 2004; Wright et al., 2009). In the Rock Canyon fault zone, laminae are parallel to fault/vein walls and their crystals grow perpendicular to the walls and toward the source of fluids (Shipton et al., 2004). No horizontally bedded travertine deposits, common where faults and fissures feed CO_2-rich fluids to the surface of the earth (Brogi and Capezzuoli, 2009; Brogi et al., 2010; Cakir, 1999; Hancock et al., 1999; Mesci et al., 2007; Uysal et al., 2009; Wright et al., 2009) were found. Travertine types include flowstone, botryoidal, bulbous and tubular varieties. Travertine deposits are also found both as clasts within breccias and as laminated rims completely surrounding breccia clasts. The following descriptions come from travertine deposits along Faults A and C.

3.2.1 Laminae and Crystal Form

Laminae on laminated travertine are distinctly visible due to the variety of colors including clear, white, tan, brown, pink, and purple. In hand sample, visible individual laminae range from 0.25 mm to 1 cm in thickness. In thin section, laminae range from 50 microns to 1.5 mm thick. The width (w) range is therefore 50 microns < w < 1 cm. The boundaries between successive laminae represent event horizons (Pentecost, 2005). Travertine in samples examined from the Rock Canyon fault zone range in number from 17 to ~1550 laminae (Figure 12a and b). The laminae in samples exhibit a pattern closely related to the growth surface. Orientation of laminae is parallel to the growth surface, forming planar bands parallel to fault walls or

concentric layers when precipitated around clasts. In a conduit, some travertine has been observed to grow from each wall inward until the void in the conduit is sealed. In some samples laminated zones that are truncated by another form of travertine are visible. The lamination found in the travertine is cyclothemic, a complex sequence of laminae displaying repetition (Figure 13; Pentecost, 2005).

All the travertine is made of acicular crystals of calcite or aragonite, referred to here as calcite. The acicular calcite found in the travertine is up to 1 cm in length and 200 microns in width. The observed long axes of the acicular crystals remain perpendicular to the lamination in the travertine**.** Crystals with this structure grow perpendicular to the fault/vein plane or clast wall.

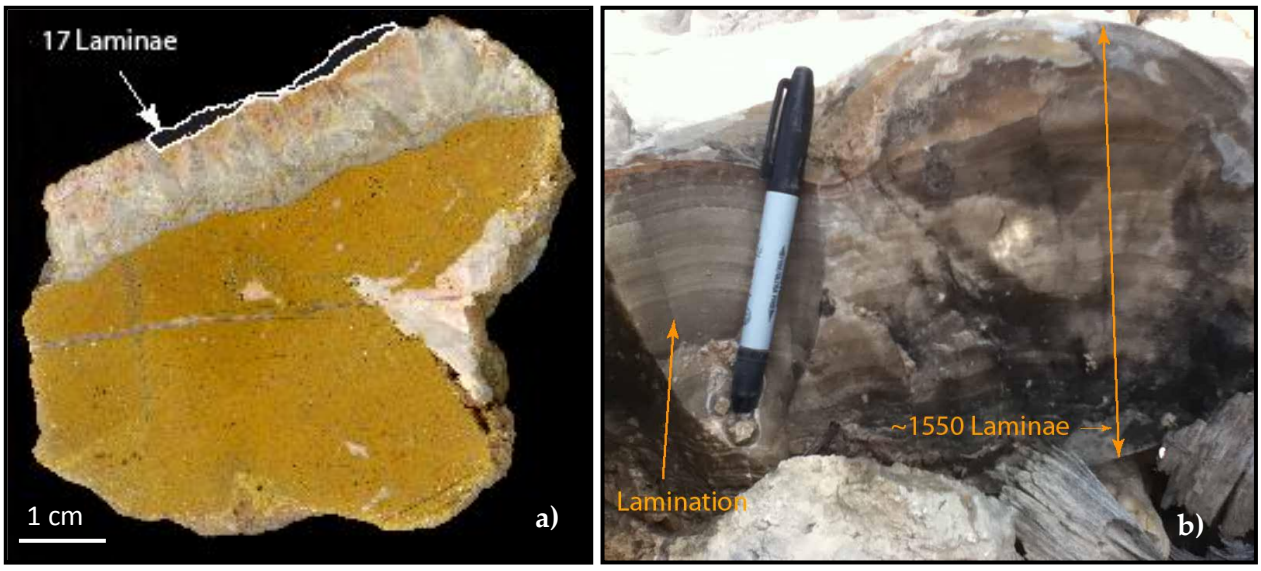

Fig. 12 *Two rocks displaying laminated travertine.* a) *Contains a thin travertine layer on the outer wall to the calcite crystals with 17 laminae.* b) *Botryoidal travertine slump found at location 25-1 with ~ 1550 laminae.*

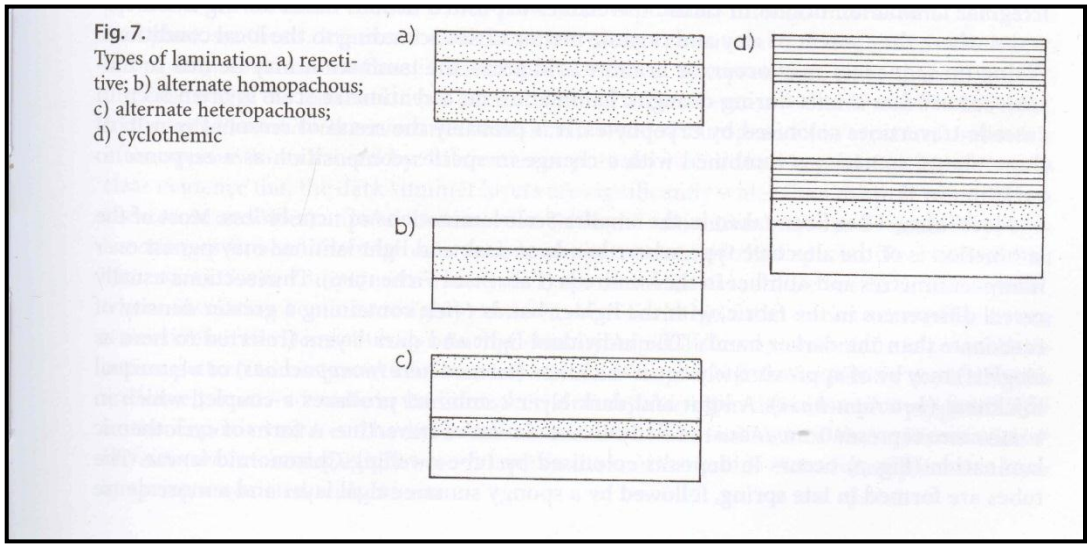

Fig. 13 *Possible lamination types foundin travertine. Samples collected from Rock Canyon fault zone displayed a mix of repetitive and cyclothemic types. Modified from Pentecost, 2005.*

3.2.2 Travertine Forms

Travertine can produce structures such as botryoidal spheres, bulbs, drip structures, and tubes (Figure 15). All these structures contain acicular crystals and laminae. Botryoidal spheres (Figure 12b and 15a) are commonly found in travertine and contain a point from which calcite crystals grow outward in all directions, forming partial spheres. Random nucleation on one of these partial spheres creates the botryoidal structure we see in some samples and is indicative of slow nucleation (Figure 14; Jettestuen et. al., 2006). Locality 24-4 and 24-5 are the only places where bulbous travertine (Figure 15b) is found. This unusual form has a nucleation point centered at the white base of the bulb. Growth moves preferentially outward into the void space concentrically but asymmetrically. The base of this form is narrow compared to its "mushroom" top. Drip structures were also found and have a resemblance to speleothems

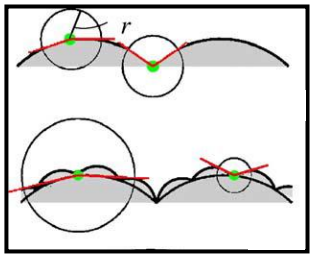

Fig. 14 *Shows cusp points at which the travertine will nucleate a new sphere. Modified from Jettestuen, 2006.*

Fig. 15

Travertine Forms

Botryoidal

a)

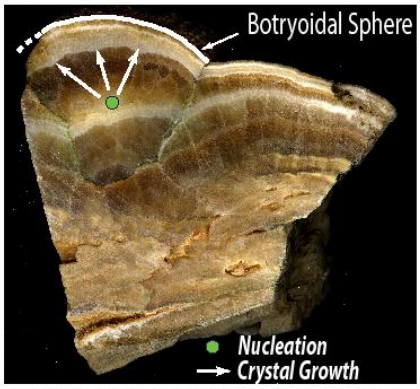

Bulbous

b)

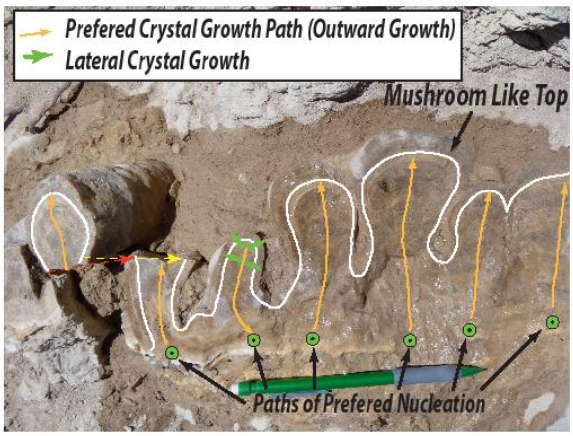

Drip

c)

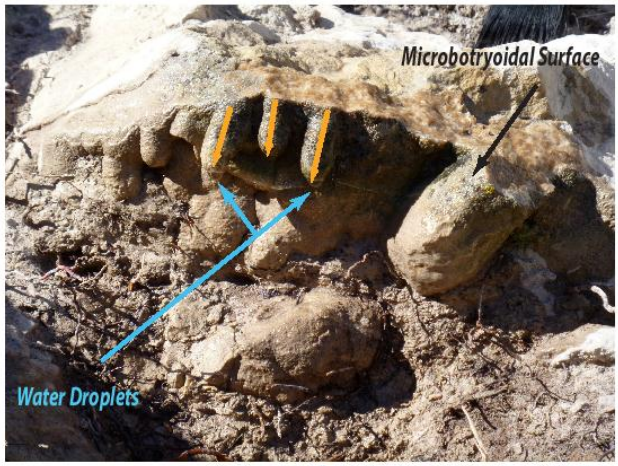

Tube

d)

e

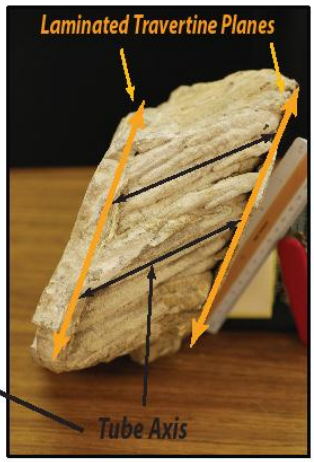

(Figure15c). The finger-like structures have a central point (center of structure) and a microbotryoidal surface. Tubular travertine was found along Fault A (Figure 15d) and B (Figure 15e). The long tube axis acts as the growth surface. Concentric layers are then precipitated growing outward into the open space around the tube. In Figure 15d multiple tubes are present and have grown to fill a 4 meter wide band within the fault zone. Some tubes occur within veins bound by laminated travertine walls as in Figure 15e. With respect to the vein walls, the bulbous travertines form perpendicularly while the drip and tube travertines form obliquely.

3.3 Calcite

Calcite in the fault zone range from hairline veins (<1 mm wide) to blocky and elongate calcite veins up to 15 cm wide. Most veins are parallel to subparallel to the fault margin. Some veins have an attitude 45 to 90 degrees to the fault margin. Rocks in close proximity to a fault margin typically display intense veining, usually hairline in size but up to 3 mm in width.

3.3.1 Blocky and Elongate Calcite

Calcite veins typically have blocky calcite and elongate calcite textures. The white to pale orange blocky calcite crystals consist of equant crystals from 2 cm to 4 cm across and fill the vein completely. Equant calcite occurs when there is continuous nucleation which is associated with supersaturation of the host fluid (Wright et al., 2009). Supersaturation can occur when the hydraulic pressure of a fluid drops, causing an increase in saturation and precipitation (Wright et al., 2009). More typically, veins are filled with elongate calcite crystals (Figure 6a and 16) that range from 0.5 – 12.5 cm long and 1 mm – 3 cm wide. Crystal long axes are oriented perpendicular to vein walls, and crystals decrease in number and increase in size from vein

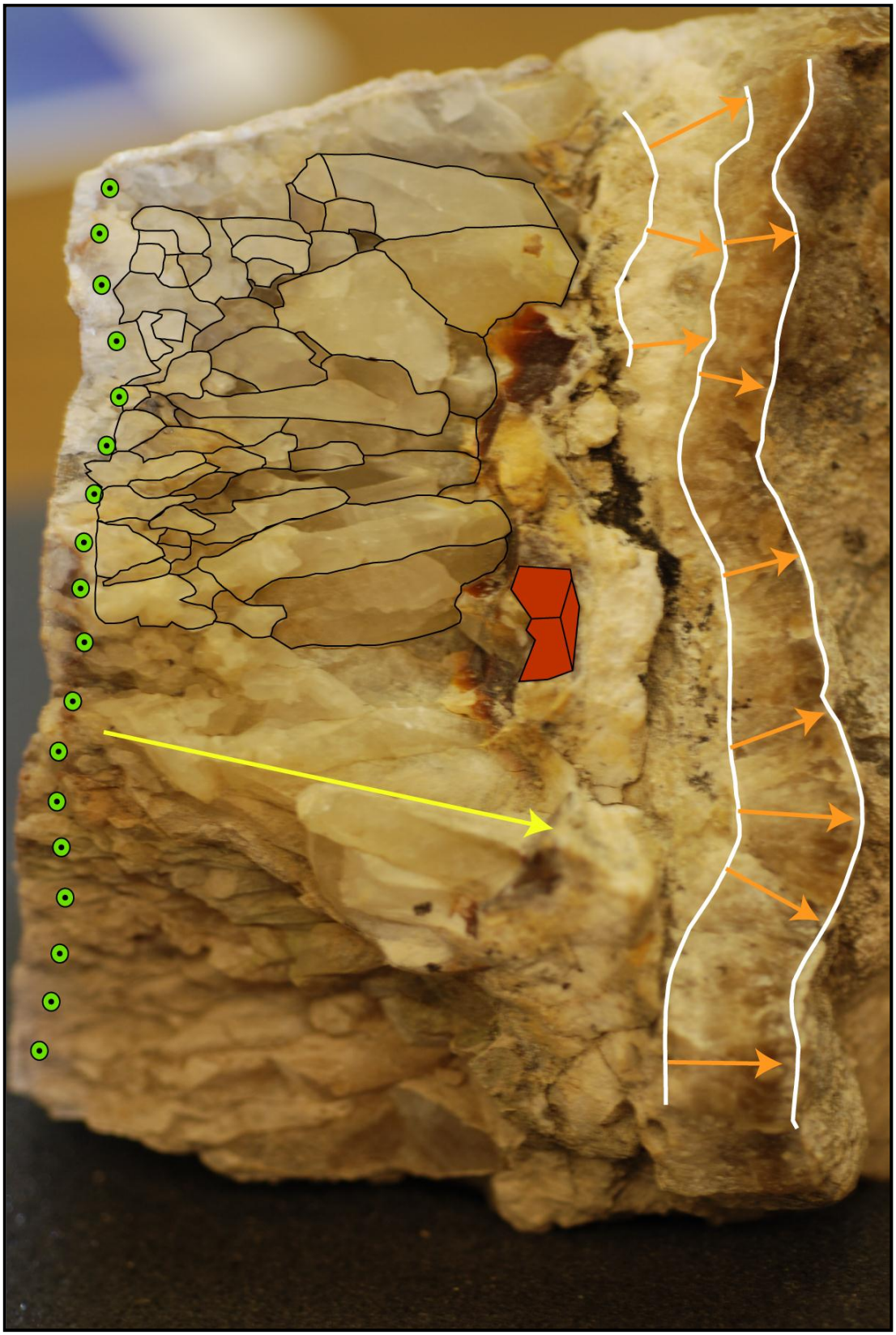

Fig. 16 *Sample 24-5, a hybrid vein deposit shows a green dotted nucleation surface, black outlined crystals, yellow calcite crystal growth arrow, red polygon hematite surface, white travertine lamination line, and orange travertine crystal growth arrows.*

walls toward the vein interior (Figure 16). This texture is characteristic of crystal growth outward from the growth surface into open/void space due to competitive crystal growth and lower nucleation rates (Wright et al., 2009).

3.4 Multiphase Hybrid Veins

These veins are composed of both travertine and elongate calcite crystals. An example is shown in Figure 16, a sample where laminated travertine, elongate calcite, and a brown-red mineral (possibly hematite) are present. Many small elongate calcite crystals grow outward from the nucleation surface (green circle with black dot). The competitive crystal growth direction (yellow arrow) is perpendicular to the growth surface and the crystals (black outlines) decrease in number and increase in size away from this surface. The calcite crystal terminations (red polygons) are coated with the red-brown mineralization. Additional vein layers occur inward from the wall, including laminated travertine (white lines) that has a growth direction (orange arrows) perpendicular to the laminae, in the same direction as the elongate calcite. The rock in Figure 16 is a multiphase vein, indicating multiple episodes of fluid flux and precipitation.

3.5 Fault Rocks and Breccias

Two breccia classifications have been proposed by Mort and Woodcock (2008), and Woodcock et al. (2006). The latter classification of breccias is done according to proportion of cement or matrix and clast concentration (Fig 17a) and reveals mechanisms for breccia formation (Woodcock et al., 2006). The former classification lumps the breccias into crackle, mosaic, or chaotic breccias according to clast concentration and average clast rotation (Figure 17b). Both classifications were used in determining the name and process of formation of the breccias in Rock Canyon fault zone.

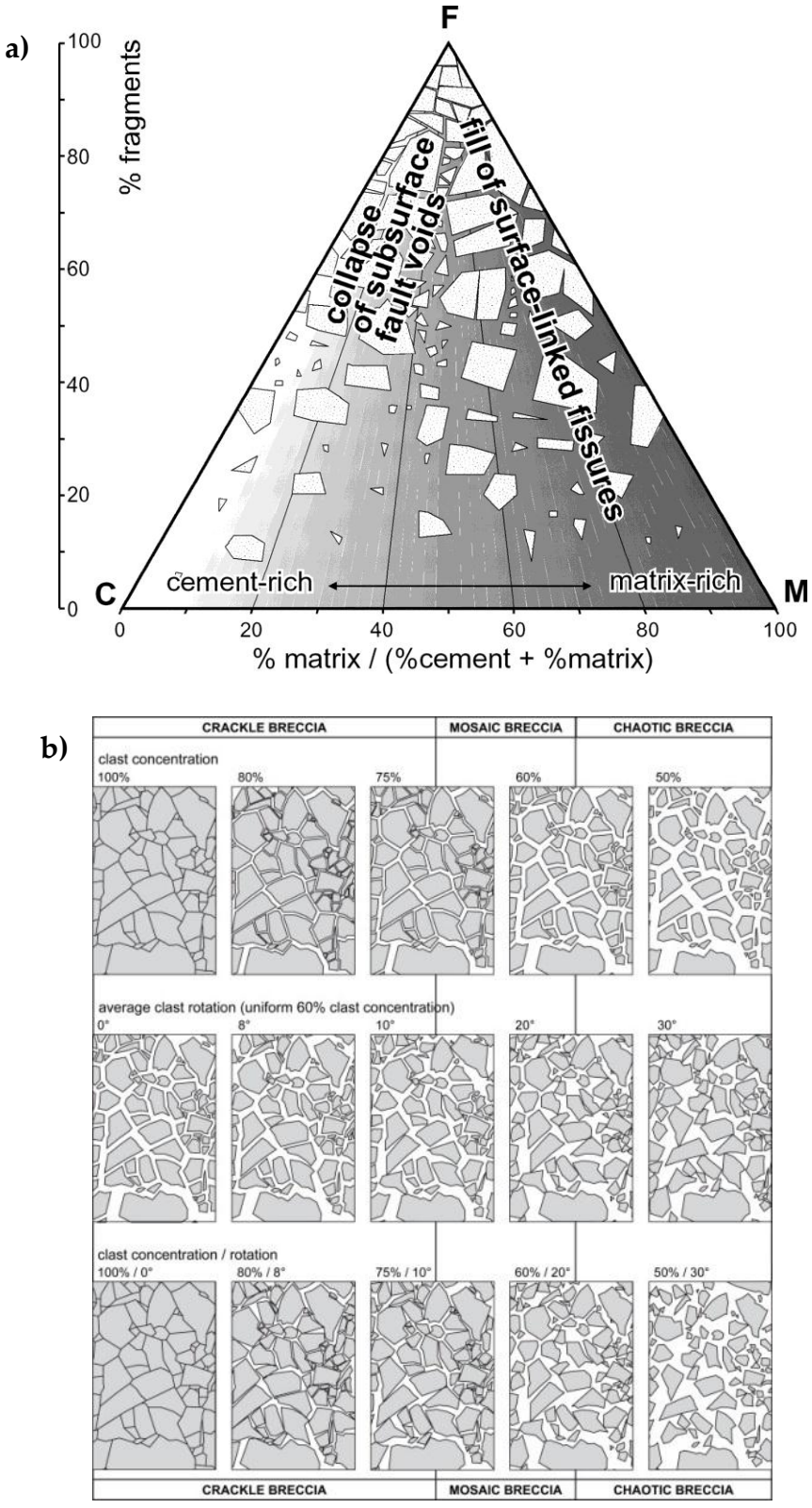

Fig. 17 *a) Breccia classification scheme proposed by Woodcock et al. (2006) based on the percentage of clasts/fragments and proportion of matrix or cement. F = fragments, C = cement, and M = matrix. b) Breccia classification scheme proposed by Mort and Woodcock (2008), based on the clast concentration and average clast rotation.*

The least strained fault rocks are crackle and mosaic breccias. In a limestone protolith, crackle breccia is pervaded by a network of small calcite veins that hardly displace the resulting fragments (Mort and Woodcock, 2008;Woodcock and Mort, 2008;Woodcock et al., 2006; Wright et al., 2009) as seen in Figure 18. In mosaic breccia, the fragments are separated and rotated but do not lose their "fitted-fabric texture" (Wright et al., 2009). The crackle breccias in the fault zone contained cement between clasts composed of calcite and are indicative of open space. No mosaic breccias were found in the study area. Three crackle breccias were recorded and one sampled. Figure 18 contains a pink-tan limestone intensely veined with calcite ranging from 10 microns to 8 mm in width. Clasts of angular limestone range from 0.5 mm to 2.5 cm in size. Veins are truncated by white, tan and brown travertine laminae (~300 laminae).

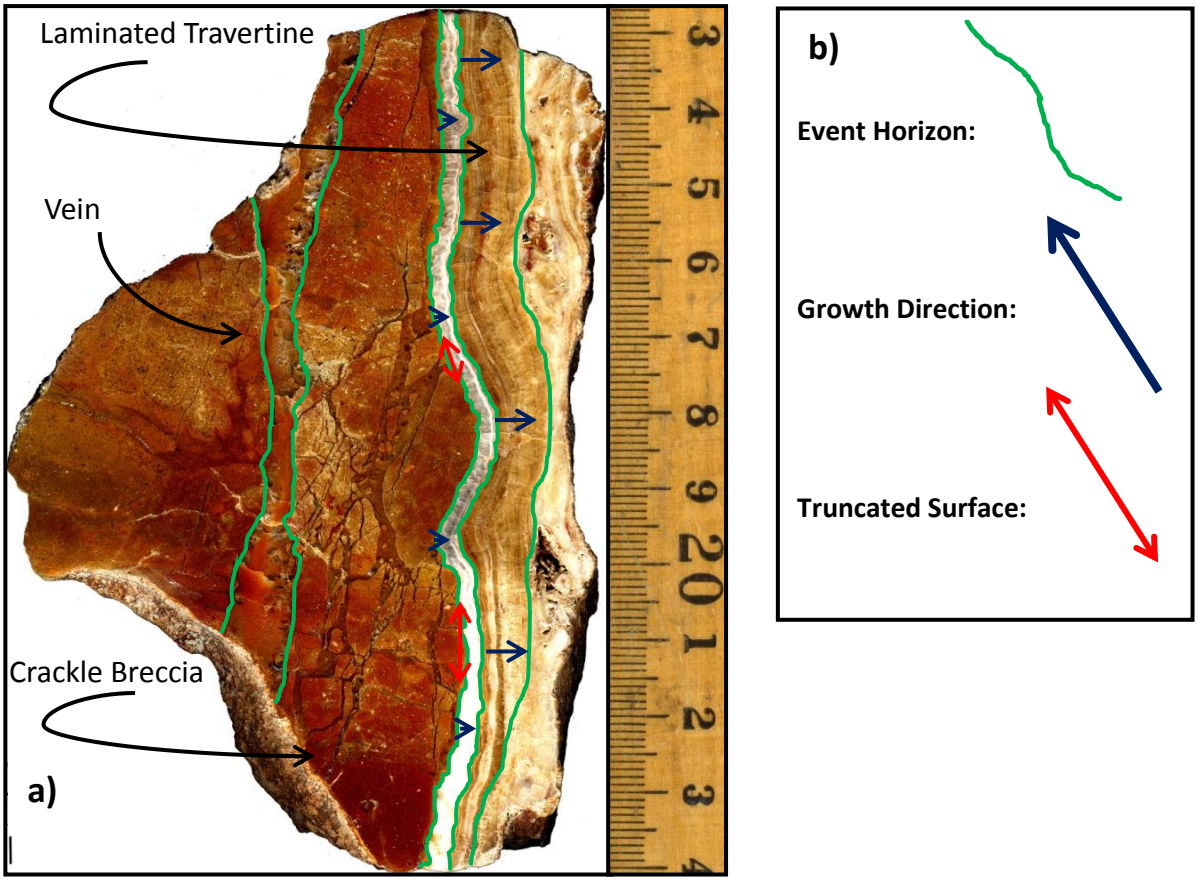

Fig. 18 *a) Sample 8b. Green lines represent event horizons, red lines represent truncations and blue arrows are the growth directions of the travertine. b) Key for Figures 18, 21, and 23.*

Chaotic breccia is composed of clasts that have been rotated enough to lose their fitted texture (Wright et al., 2009). Breccias of this category found in Rock Canyon fault zone display a wide range of clast types, including siltstone, limestone, sandstone, laminated travertine and calcite. The primary cements are calcite and travertine. Some clasts are completely surrounded by travertine, and their size ranges from 1mm – 17 cm in diameter. Unique breccias, cockade breccias, are formed during fracturing events where clasts rotate during shearing to create discontinuous patterns (Leroy et al., 2000). In the eastern region of the Rock Canyon fault zone show a nucleus of pink laminated travertine or tan laminated travertine surrounded by brown laminated travertine (Figure 19). Four chaotic breccias from Fault A are examined in detail in the following sections.

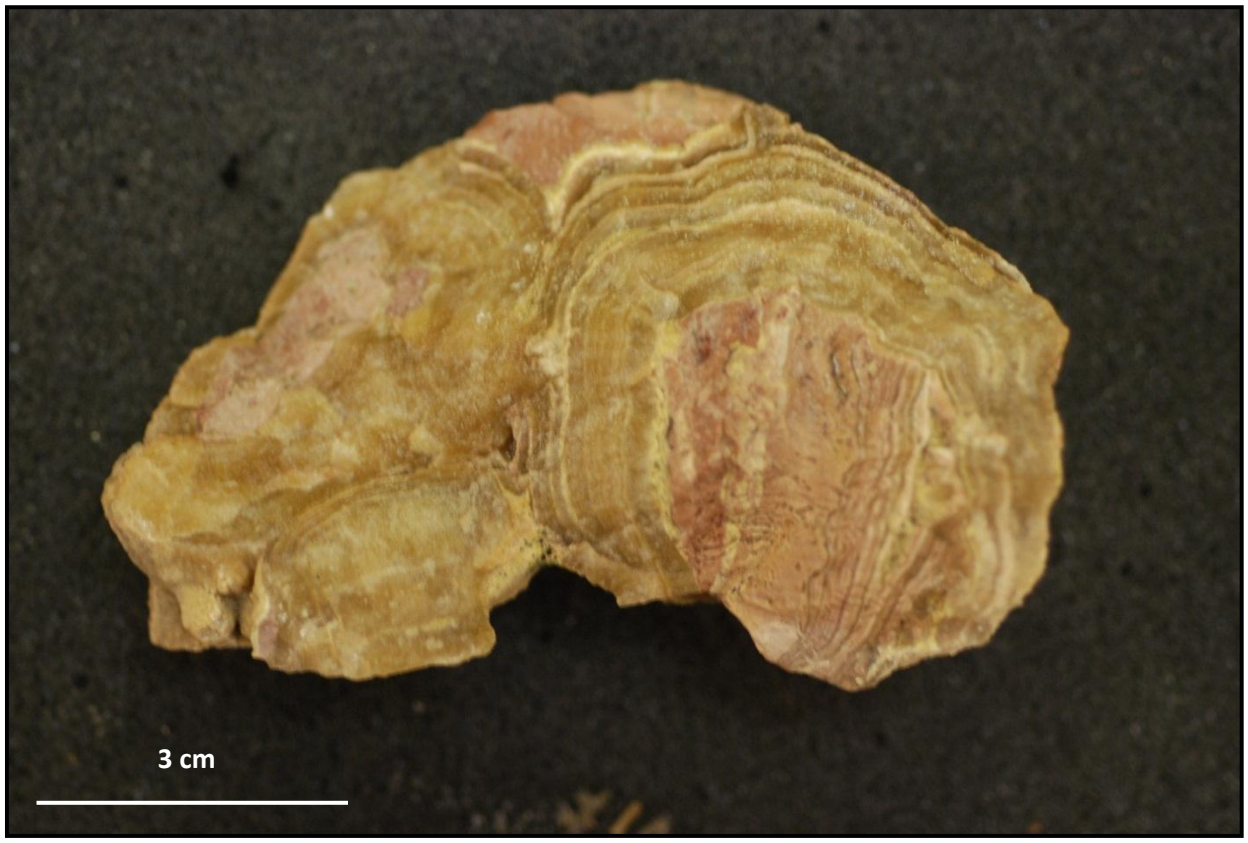

Fig. 19 *Sample of cockade breccia containing three nuclei. The nuclei consist of tan laminated travertine and pink laminated travertine surrounded by brown laminated travertine.*

1. Sample 25-4 (Figure 20) is the easternmost sample. It exhibits voids of open space ranging from 1 mm to 2 cm in diameter (~10% of rock). The angular clasts are supported by travertine cement, range in size from 2 mm to 4.5 cm, and have a composition of calcite, limestone, siltstone, and breccia. 25-4 contains four superimposed breccias (Br_{1-4}) with Br_1 being the oldest and Br_4 being the most recent. The dark grey breccias (Br_1) contain calcite and black minerals that cannot be identified in hand sample. The limestone breccia clasts (Br_2) contain truncated calcite veins and clasts of Br_1. Br_3 has a travertine cement with clasts of both Br_1 and Br_2. Br_4 is the whole sample and contains all other breccias. This sample thus represents four generations of breccia formation.

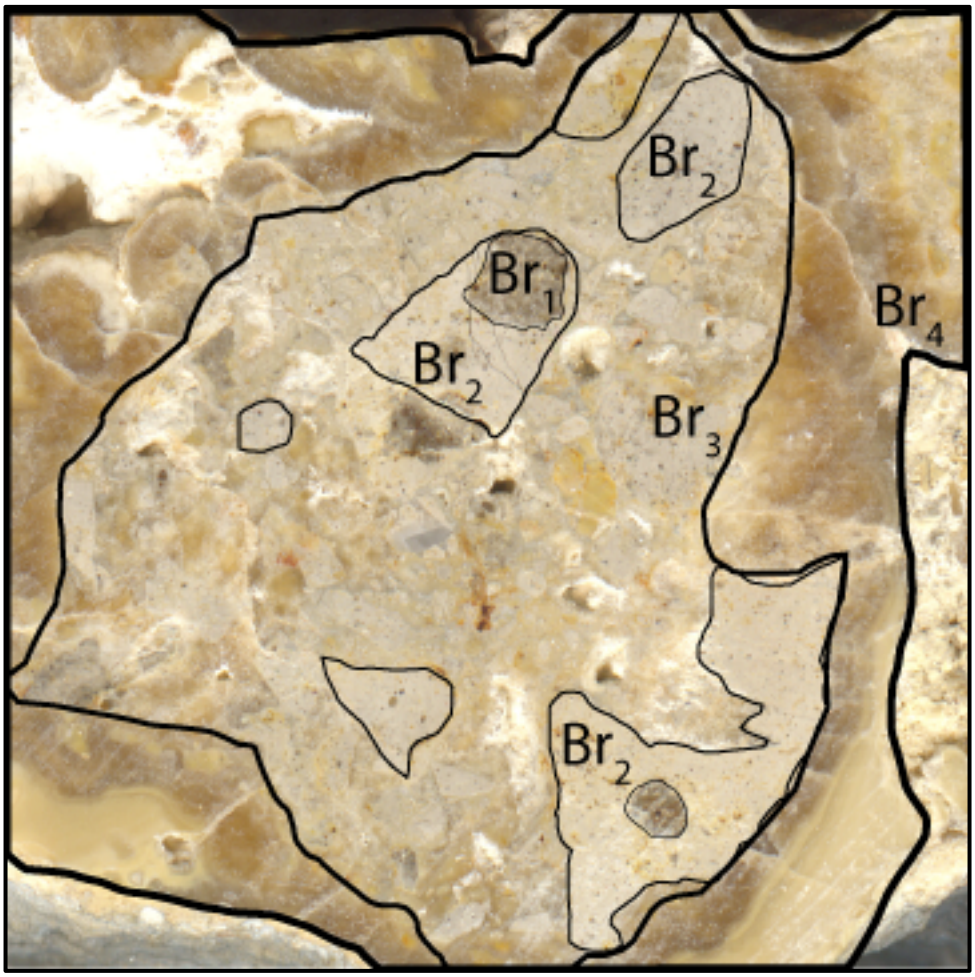

Fig. 20 *Limestone clast in sample 25-4 containing three superimposed breccias. This clast is in a travertine cement supported matrix in one of the explosive breccias.*

2. Sample 9 (Figure 21) contains less than 3% voids that range from 1 mm to 4 mm in diameter. Sample 9 contains angular to subangular clasts and is clast supported with possibly a micrite cement (thin section of rock is required to fully identify cement). Clasts range in size from 1 mm to 2.5 cm in diameter and have a composition of siltstone, calcite, limestone and breccia. Breccia 1 (Br_1) contains calcite and unidentifiable black lithics. Breccia 2 (Br_2) contains angular clasts of siltstone, limestone, calcite and Br_1. Breccia 3 (Br_3) contains calcite, siltstone, limestone, Br_2 and Br_2. Br_3 is surrounded on three sides by a laminated, then acicular calcite.

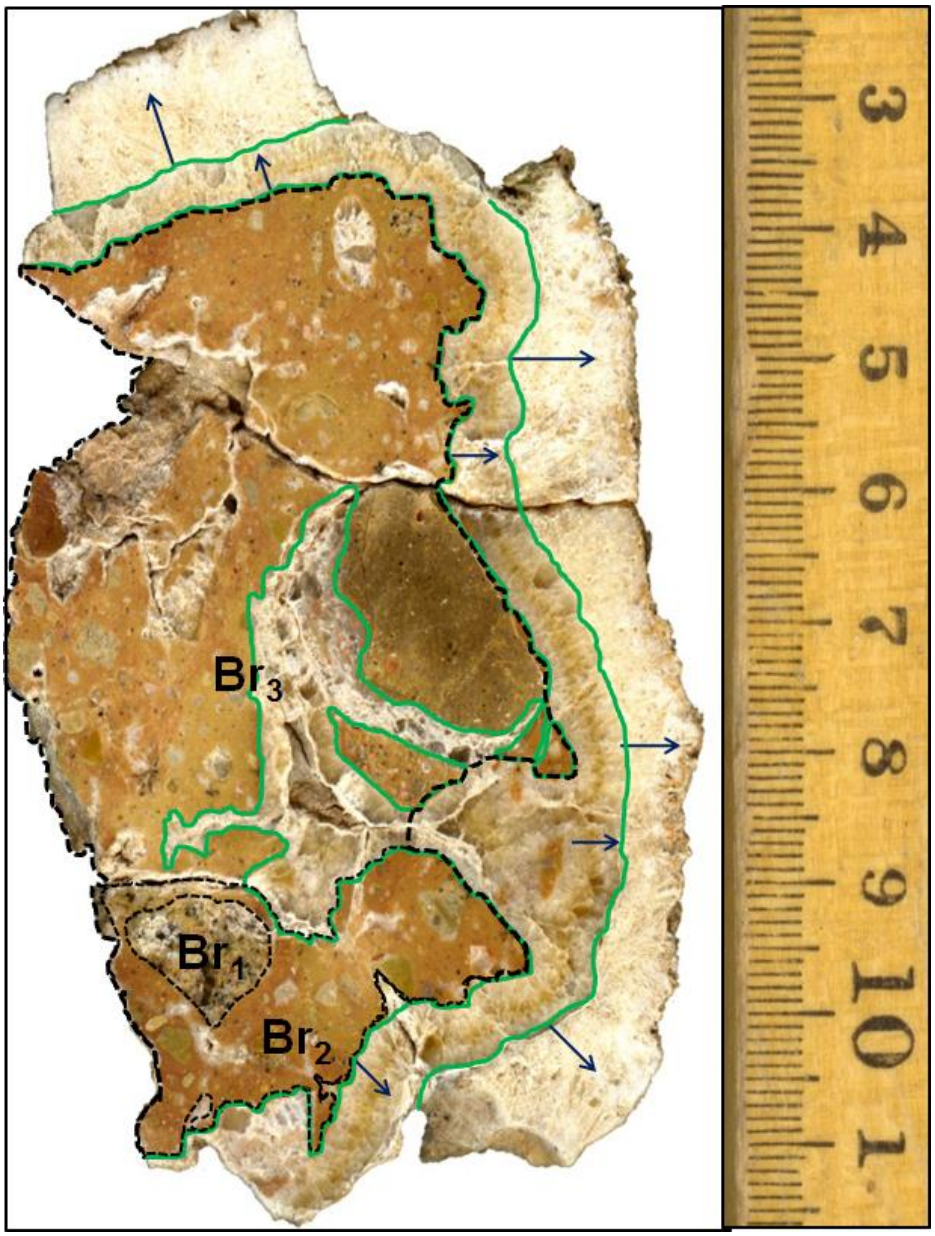

Fig. 21 *Sample 9 with 3 superimposed breccias (Br_1, Br_2, Br_3) and two forms of calcite surrounding most of the Br_3 clast.*

3. Sample 6a (Figure 22) contains less than 1% voids that are less than 1 mm in diameter. Angular calcite clasts (C) support breccia with calcite cement, ranging in size from 1 mm to 2 cm in diameter, and are mainly composed of calcite crystals with sparse veined siltstone.

Fig. 22 *Sample 6a is a chaotic calcite breccia. This breccia is composed mainly of calcite clasts (C) with sparse siltstone fragments and contains a calcite cement.*

4. Sample 6c (Figure 23) contains less than 1% voids that range from 1mm to 2mm in diameter. Angular to subangular clasts are calcite cement supported with small amounts of red micrite, range in size from 1 mm to 2.5 cm in diameter, and have a composition of calcite and siltstone. A portion of the rock contains euhedral calcite crystals laced with a black mineral, possibly hematite.

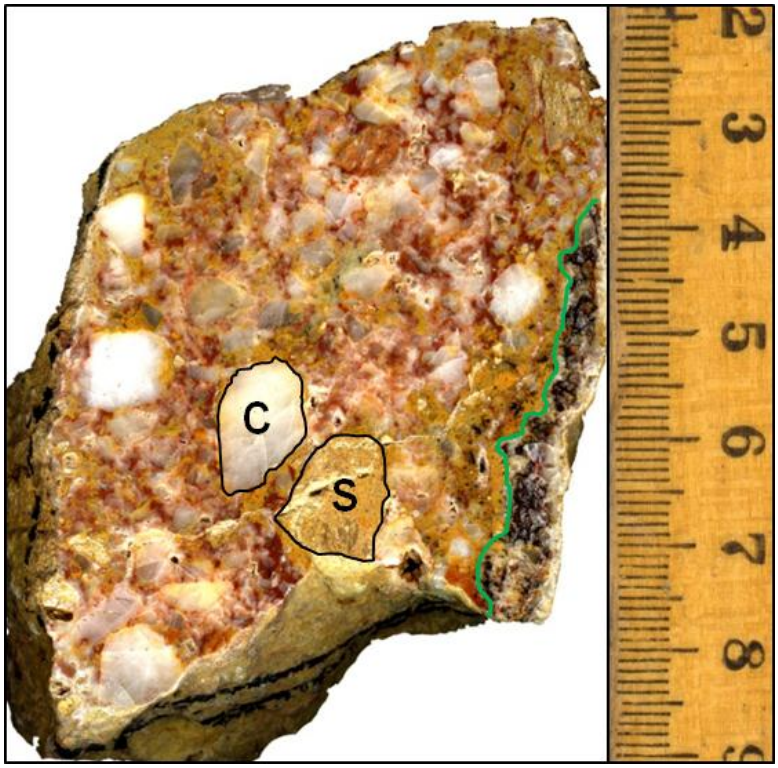

Fig. 23 *Sample 6c with clasts of calcite (C) and siltstone (S) in a calcite matrix.*

3.6 Structural Analysis

Measurements were taken in the field of fault planes, fault-parallel veins, veins, and tube long axes within tubular travertine zones. Fault types, including planes with stratigraphic offset (F), breccia margins (F_B), planes with slickenlines (F_{SL}), planes with slickenfibers (F_{SF}), and a hybrid (F_H) of planes with slickenfibers and crystalline calcite, were measured and plotted. Fault-parallel veins were classified as laminated travertine veins (FPV_T), crystalline calcite veins (FPV_C), and a combination of both (FPV_H). Veins were classified as opening-mode veins that have fibers perpendicular to vein walls (V_{OM}), calcite-filled veins with crystals that grew into open space (V_{COS}), laminated travertine veins that are not fault related (V_{LT}), and veins composed of both laminated travertine and elongate calcite (V_H).

Five stereoplots were produced by combining structure types together (Figure 24). The bold red line is the average attitude of Fault A (N83E, 71S) as measured by the 3-point problem.

Travertine veins around Fault A (brown) and Fault C (green) are oriented generally E-W and N-S, with a considerable scatter in orientation (Figure 24a). The east-west trend is parallel to the main fault orientation, whereas the north-south veins are subperpendicular. Fault-related travertine veins and hybrid travertine and calcite veins from Faults A (black) and C (blue) are shown in Figure 24b. Along Fault C, these veins strike E-W and dip steeply to both north and south, suggesting a conjugate set. Fault A has veins striking ENE-WSW, most dipping steeply to the south, parallel to the fault dip. A subset of veins have shallow dips to the NNW between 21 – 43 degrees. The contours show and average vein attitude trending east – west and dipping steeply to the south. Fault-related calcite veins from Fault A (black) and C (blue) (Figure 24c) strike between ENE-WSW and ESE-WNW, with very steep northerly dips most common. The contours show an average vein attitude striking east - west with a high angle dip to the north. The attitude of the long axes of travertine tubes from Fault A are shown in Figure 24d. The great circles are the planes the tubes lie within. The contours are of the long axes of the tubes with a concentration falling on the measured fault plane at an oblique angle of 20 – 50 degrees southwest.

All the fault types from Faults A, B, C, E, and F and the measured attitude of Fault A (red) are plotted on Figure 24e. Faults strike from NE to NW, with considerable scatter. Most faults dip south, parallel to the attitude of Fault A as mapped, but north-dipping faults are also present. This pattern suggests conjugate faults, probably mesoscale fault sets associated with the mapped faults, were measured. Some striae on fault planes have near dip-slip orientations, ranging from 78 – 89 degrees in pitch. The majority of measured striae range from 23 to 38

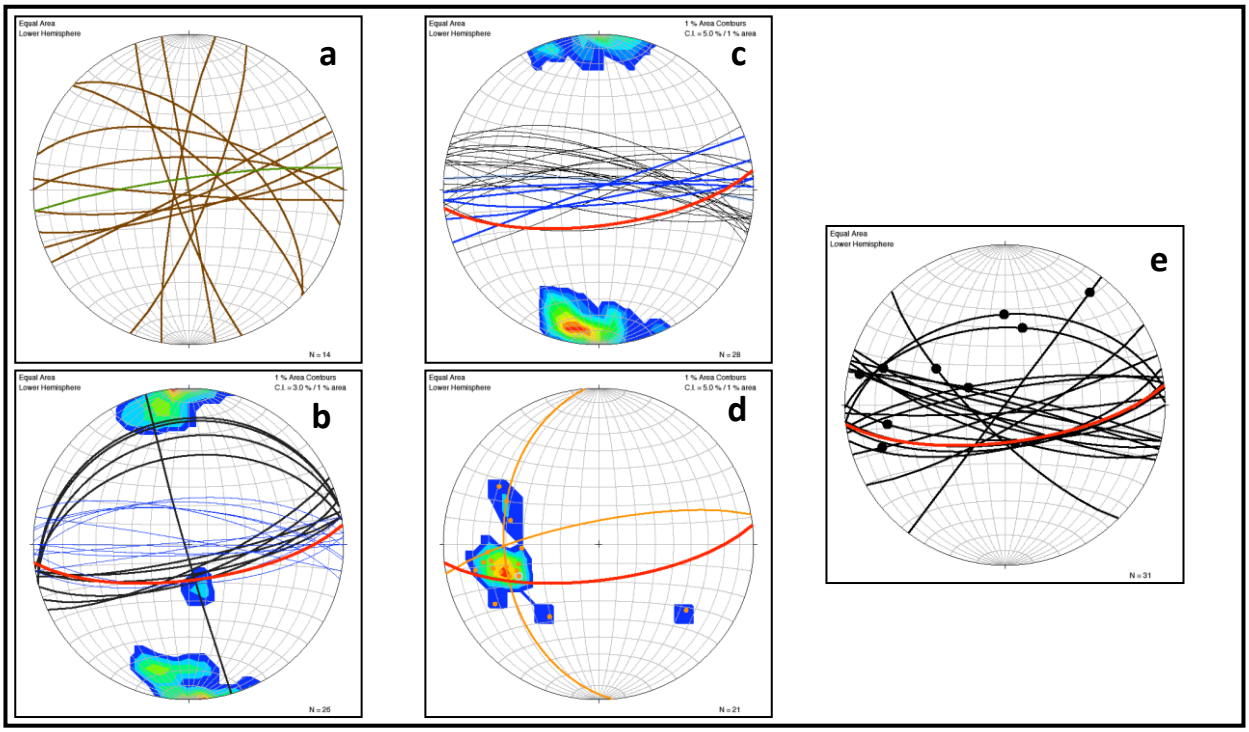

Fig. 24 *Structural data plotted in Stereonet with average fault attitude of N83E, 71S (red).* ***a)*** *Veins around Fault A and C with considerable scatter orientation.* ***b)*** *Fault-related travertine veins and hybrid travertine and calcite veins from Faults A (black) and C (blue).* ***c)*** *Fault related veins from Fault A (black) and C (blue).* ***d)*** *Yellow lines are planes with long axis (dots) of travertine tubes from Fault A.* ***e)*** *All fault types from Faults A, B, C, E, F with some plane and pitch attitudes (black dots).*

degrees west in pitch within the measured fault plane. Although the population of measured striae on faults is small, they appear to be on average parallel to the long axes of tubes within tubular travertine zones within Fault A.

4. Discussion

4.1 Fault Orientation and Kinematics

The fault zone contains faults and veins that are oriented nearly parallel to each other, on average striking east – west. Fault B is the best exposed north-dipping normal fault, with a dip angle of 43-50 degrees. According to Figure 24e there are north-dipping faults, other than Fault B, that range from 78 to 88 degrees north. All other faults dip between 70 and 88 degrees south.

This fault pattern is similar to conjugate geometry but the angle between the faults is smaller than Coulomb-Mohr theory predicts. The veins in the zone have northward and southward dips, suggesting a conjugate fracture network. The close orientation of both faults and veins suggests us that one stress regime acted on this zone to create these parallel structures. Laminated travertine veins found between faults are both parallel and perpendicular to the mapped faults. In some cases the veins perpendicular to the fault cut the veins parallel to the fault. These veins are therefore younger in age and possibly represent a separate stress regime.

Rock Canyon fault zone has a normal stratigraphic dip separation component of 260 meters, but contain faults with normal or oblique slip directions due to the presence of slicken lines and fibers with steps on 3 faults. Some faults show both normal and oblique motion indicating two separate slip events. The oblique-slip faults associated with mapped Faults A, C, and F contain slip lineations with pitches of 13- 64 degrees west and slip-sense indicators that reveal right-lateral, normal motion. This motion would drop the graben block down and to the west. However, Fault E displays a pitch of 22 degrees west with slip indicators of left-lateral reverse motion that would bring the graben block up and to the east. Slickenline/fiber surfaces were scarce and therefore few attitudes were taken on faults with sense indicators. The sparse data limit the conclusions that can be drawn. Stratigraphic offset documents normal, down-to-the-south separation of 260 meters, consistent with the down-dropped graben morphology. Some slickenfibers/lines were found on Faults A, B, and C, with pitchs ranging from 70 – 87 degrees west, with a normal motion sense, consistent with the stratigraphic separation and morphology. It is unclear from the present data whether oblique-slip contributed to producing the stratigraphic separation, or whether there were two different, successive types of motion that occurred on the

fault, such as normal slip followed by oblique slip. Further field data is required to resolve fault kinematic history.

4.2 Brecciation and Precipitation Processes

Based on analogies with similar breccias described elsewhere, there are two processes that are interpreted to have formed the breccias seen in Rock Canyon fault zone. Uysal et al. (2009) discuss the formation of explosive breccias. Lowering the water table during dry periods leads to higher levels of CO_2 in deep water reservoirs because of the reduction of surface discharge (Uysal et al., 2009). Oversaturation of these reservoirs can lead to rapid exsolution of CO_2 gas that then expands and accelerates rapidly upward under its high buoyancy causing explosive fracturing of the walls of the conduit (Uysal et al., 2009). The quick release of pressure as the fluid gas migrates toward the surface causes quick precipitation, locking the clasts in a $CaCO_3$ cement (Uysal et al., 2009). Sample 25-4 has angular clasts surrounded by travertine precipitated on all sides, and could exemplify one of these explosive breccias.

The second process is fault void fill as a result of fracturing during slip along irregular fault planes, as described in Woodcock et al. (2006). Figure 25a shows a reverse fault in cross section before slip. This same process could apply to the normal fault kinematics along the Rock Canyon fault zone. As the hanging wall progresses upward a void is formed (Figure 25b) and hydrothermal flow through the void begins (Woodcock et al., 2006). Rocks on the hanging wall begin to implode and collapse (Figure 25c) filling the void along the fault, and hydrothermal fluid flow begins to cement the breccia clasts (Woodcock et al., 2006). Eventually the void is

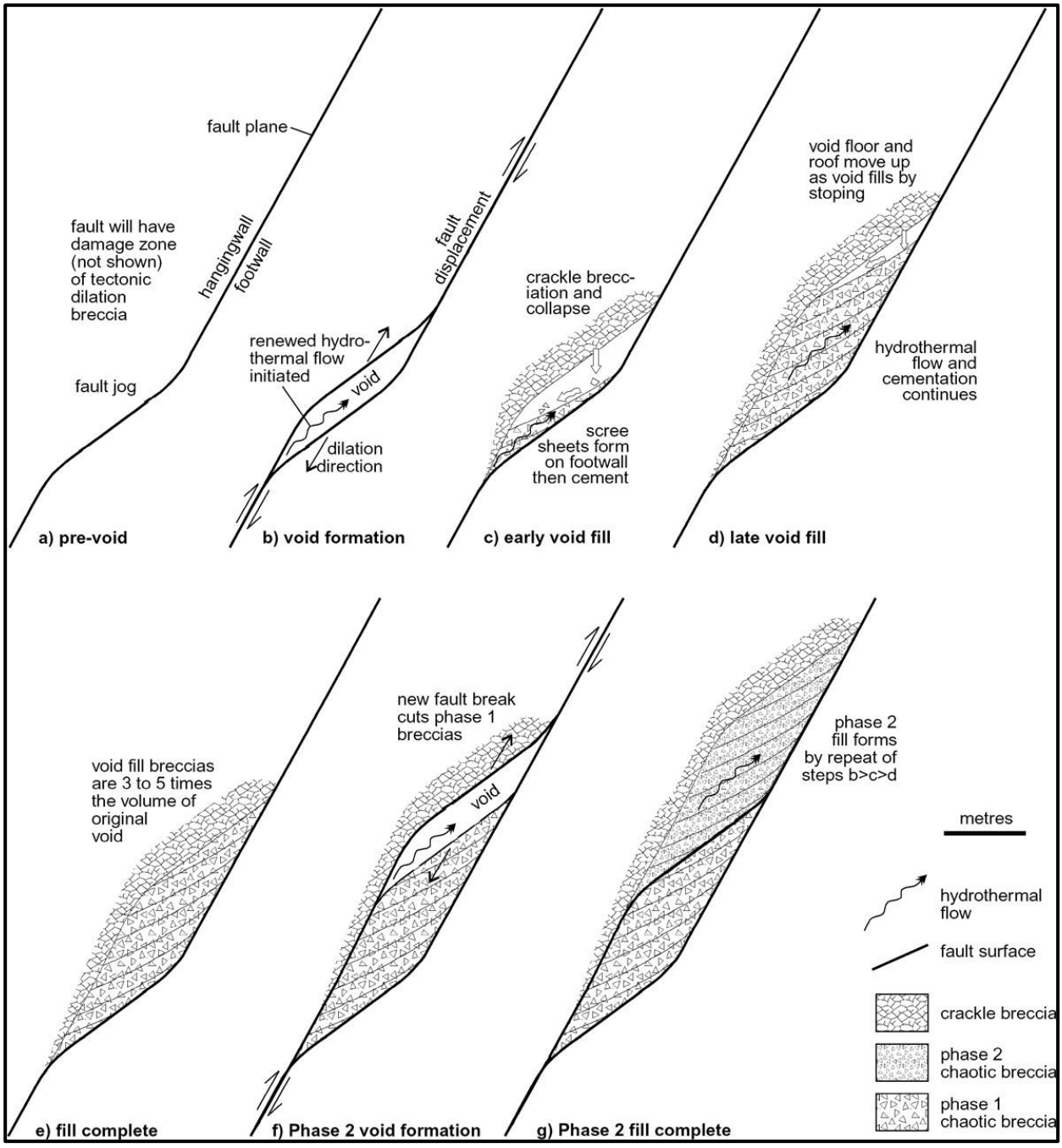

Fig. 25 *Schematic infill of fault void due to implosion of the hanging-wall and precipitation of carbonate through hydrothermal flow. From Woodcock et al. (2006).*

choked with collapsed breccia (Figures 25d and e). The fault then slips again creating a second void (Figure 25f), c and d are then repeating to create g (Figure 25g). Samples 6a and 6c are clast-supported breccias that could represent void fill breccia formed by this process.

The CO_2 to drive precipitation of $CaCO_3$ has its source in deeply seated carbonate reservoirs. The fluid in these reservoirs seeps through conduits (open space) such as permeable rock lithologies or fault/fracture openings in the rock. As the fluid migrates upward pressure on the fluid is released causing precipitation in the conduit. Through field observations we know travertine and calcite are precipitated in bands on the steeply-dipping fracture surface(s) and grow perpendicular to this nucleation surface. Eventually, the fracture is sealed preventing the fluid from reaching the surface. The fracture seals when the precipitate from one wall of the conduit reaches the other, or when nucleation and growth from each side of the vein meet in the center and seal the fracture. The multiple phases of fault-parallel veining observed indicates repeated episodes of fracturing, fluid flow, precipitation and sealing.

In some cases the bands within the fault zones were filled with tubular travertine. In Figure 24d the tube orientation falls on the fault plane at an oblique angle to the west. In Figure 24e the slickenfibers/lines are at an oblique angle within the fault planes and have the same range in attitude as the tubes. This evidence suggests that the tubes formed syntectonically. By analogy with fibrous veins, continuous fluid flux while a fracture gradually opens and slips likely produced the oriented, elongate travertine tubes. Precipitation of the range of types observed are typical of near-surface deformation processes, where low lithostatic pressures permit open space to form.

4.3 Fault History

Detailed maps and fault-rock samples document multiple brecciation and precipitation events. In Figure 5 the three calcite veins are growing from the north to the south with breccia in the southeast corner of the map. On each vein crystal growth termination represents a successive precipitation pulse. Figure 7 shows calcite then travertine precipitation events, followed by brecciation and calcite precipitation. Figure 8 contains two large travertine precipitation events and one brecciation event. As mentioned in the results section the factors controlling the development of the travertine laminae cannot be determined without further investigation into the isotopes they contain.

Figures 18a, 20, and 21 have event horizons and show record of several brecciation events. Figure 18 (Sample 8b) was slightly fractured into a crackle breccia that then filled with calcite. The rock was then broken again, as evidence by the truncation of veins by travertine, and travertine precipitated through the large fracture. Figure 21 (Sample 9) contains three breccias Br_1, Br_2, and Br_3. Br1, created by a slip event, is inside of a Br_2 with clasts of angular calcite. Br_2 is inside of Br_3 which also contains angular calcite clasts. The outside of Br_3 has a laminated calcite and acicular calcite. The evolution of this breccia starts with a slip event (Br_1) and precipitation of calcite (presence of angular calcite in Br_2). Another slip event occurs (Br_2) to create a chaotic breccia. The last slip event occurs (Br_3) to create a crackle breccia that is then surrounded and filled with laminated calcite. The last precipitation event occurs, with acicular calcite almost completely surrounding the clast. This rock records three alternating brecciation and fluid pulse events. Figure 20 (Sample 25-4) contains four superimposed breccias. After three slip events, a final explosive brecciation event caused the clasts to be completely surrounded by travertine. All the samples indicate that brecciation and precipitation alternated in the fault zone.

Figure 26 depicts the Rock Canyon fault zone as it has evolved through time. Figure 26a is an illustration of the fault zone formations. Paleogene Colton (Pgc), Paleogene Flagstaff (Pgf), and Cretaceous/Paleogene North Horn (PgKn) formations are represented as horizontal with actual bedding dip ~5 degrees to the west. Jurassic Twist Gultch (Jtg) contains bedding dipping ~ 36 degrees NE creating an angular unconformity between PgKn and Jtg with thinning of PgKn to the south. The thinning is evidence of a paleohigh (Jtg) followed by PgKn, Pgf, and Pgc deposition. Figure 26b is the first faulting event that creates a void partially filled with imploded angular fragments from the hanging wall. Hydrothermal CO_2 fluid then percolates through the conduit (void) enclosing the angular fragments into a breccia (Br_1) with travertine cement (Figure 26c). A repetition of the process (b) and (c) creates a breccia (Br_2) with angular fragments from host formations and fragments of Br_1 (Figure 26d). Two alternating brecciation and precipitation events occur after (d) to create the last breccia (Br_4) (Figure 26e). Br_4 contains four superimposed breccias that record four brecciation events intermittent with travertine precipitation as seen in Sample 25-4.

4.4 Basin and Range Province

The Rock Canyon faults progressively widen from west to east as they approach a major north-south Basin and Range fault, the Valley Fault. Travertine becomes dominant in the fault zone near the junction between the east-west Rock Canyon fault zone and the north-south Valley fault. Travertine has been mapped along the Valley fault to the north of the study area (Fong, 1995; Lawton and Weiss, 1999). These relations suggest that the Rock Canyon fault and the Valley fault are structurally linked, with maximum fluid flux and travertine precipitation at their intersection. This hypothesis can be tested through analysis of the age and isotopic compositions of the travertine on both the Valley and Rock Canyon faults.

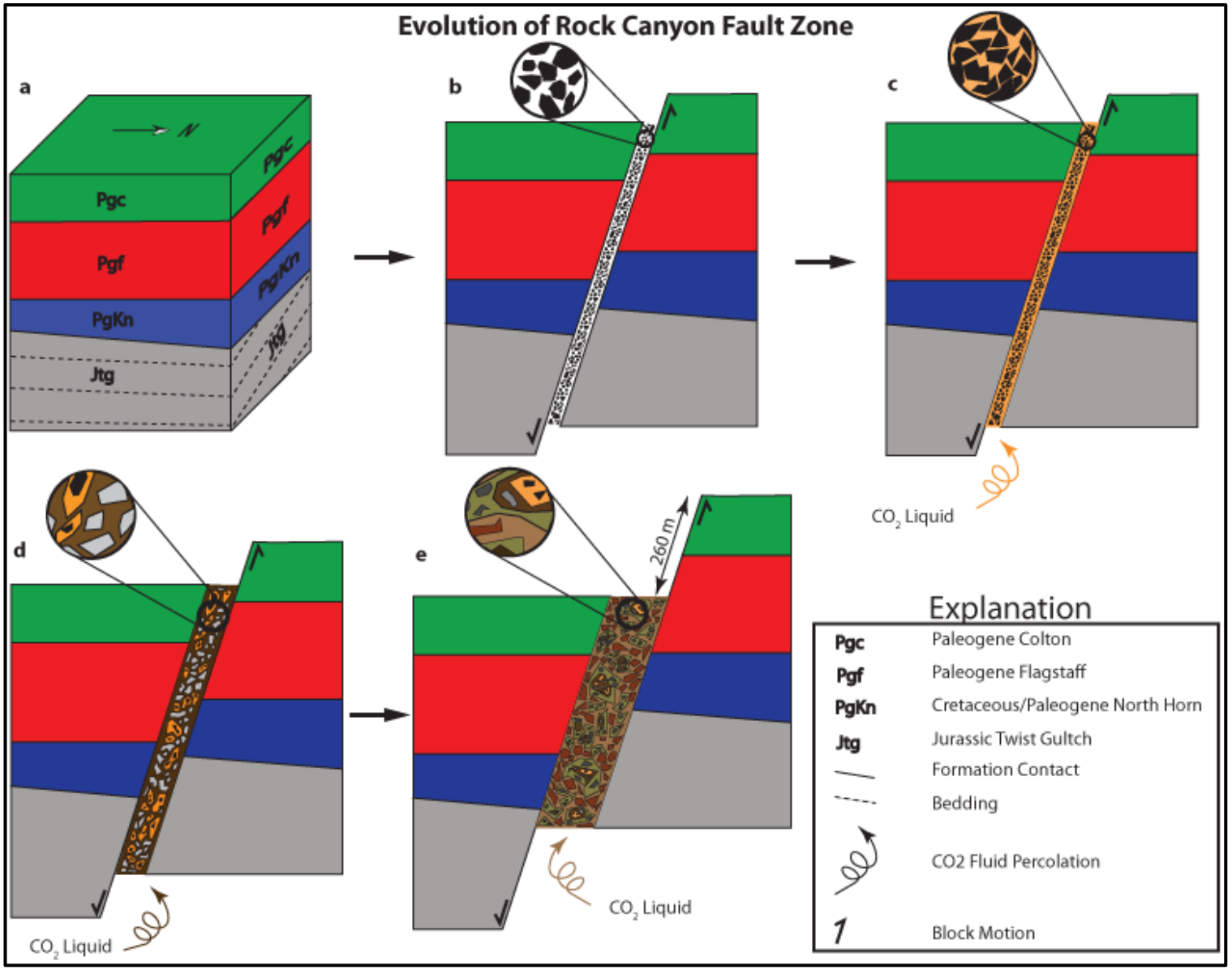

Fig. 26 *Diagram of the evolution of Rock Canyon fault*

5. Conclusions

The Rock Canyon fault zone is composed of faults, veins, breccias, and travertine deposits, all of which help to determine how this zone has evolved. The orientation of the related faults and veins trend dominantly E-W parallel to the Rock Canyon fault zone and are interpreted to have formed under the same stress regime. The travertine veins that are perpendicular to the fault zone and cut E-W veins may have formed in a different, younger stress regime. Cross section work shows there has been a normal stratigraphic dip separation of 260 meters. It is inconclusive as to how much of that slip is normal, oblique left lateral or oblique right lateral, and more structural data is needed.

We have identified two brecciation processes that can account for the rocks observed at Rock Canyon. Voids created by movement of irregular fault surfaces and filled with angular clasts from the hanging wall create the clast supported breccias sampled on the faults. Breccias with clasts completely surrounded by travertine likely formed due to explosive outgassing of liquid CO_2 gas that rapidly precipitated the breccia clasts in place. Precipitation of calcite and travertine occurred in layers parallel to steep fault walls, and were sealed by crystal growth nucleated on one or both walls. Tubular travertine with long axes oblique to fault walls formed syntectonically by continuous precipitation as the fault slipped and opened. The evolution of the fault involved multiple slip and precipitation events.

There is a connection between Rock Canyon Fault and the major north-south Basin and Range fault bounding the Sanpete Valley. The widening of the Rock Canyon fault zone toward the Valley Fault, and the change in composition from calcite to travertine, is an indication that the Rock Canyon Fault is connected to the Valley Fault. Both were conduits for fluid flow.

Further study needs to be done to better constrain the sense of motion of the fault blocks across the Rock Canyon fault zone, determine source of the fluids, age/climate of the travertine deposits, modes of formation, and relation of the Rock and Dry graben to the Basin and Range Province.

5.1 Future Work

Future work to expand this study should include more field mapping, field structural data for kinematic analysis, and sample collection for observation and isotopic data analysis. Rock Canyon Fault should be mapped in more detail, with more focus on finding slip lineations and sense indicators. Collection of ideal samples for isotopic data analysis should occur on both Rock Canyon Fault and Valley Fault, and used to compare the ages of the travertine on the Rock Canyon Fault with the ones on the Valley Fault. In an ideal situation, we would be able to determine if the faults occurred simultaneously and therefore under the same stress regime that created the Basin and Range Province. Other isotope work could include determining the source of the CO_2 saturated liquid, temperature of the atmosphere at the time of deposition (paleoclimate), and if bulbous or other travertine is microbially mediated (Chafetz and Folk, 1984; Pentecost, 2005).

Travertine contains a plethora of information that can be extracted in numerous ways. Travertine deposits are used to find locations of potentially hazardous faults (Brogi et al., 2010; Cakir 1999). Studying the isotopes within travertine or its laminae can reveal the paleoclimate in the region of the travertine and/or source of CO_2 fluid or CO_2 saturated liquid (Minissale et al., 2002; Ortner, 2003; Shipton et al., 2004; Uysal et al., 2007; Zentmyer et al., 2008). Laminations have the potential to represent bidiurnal and diurnal changes in temperature (day and night),

seasonal temperature changes, and longer term changes of solar cycles for 11, 80, and 90 years which affect travertine precipitation rate (Pentecost, 2005). Relationships between climatic change and seismic activity with respect to travertine deposition offer a better framework for neotectonic studies.

References

Chafetz, H.S., and Folk, R.L., 1984, Travertines; depositional morphology and the bacterially constructed constituents: Journal of Sedimentary Research, v. 54, p. 289-316, doi: 10.1306/212F8404-2B24-11D7-8648000102C1865D.

Dockrill, B., and Shipton, Z.K., 2010, Structural controls on leakage from a natural CO2 geologic storage site: Central Utah, U.S.A. Journal of Structural Geology, v. 32, p. 1768-1782, doi: 10.1016/j.jsg.2010.01.007.

Faccenna, C., Soligo, M., Billi, A., De Filippis, L., Funiciello, R., Rossetti, C., and Tuccimei, P., 2008, Late Pleistocene depositional cycles of the Lapis Tiburtinus travertine (Tivoli, Central Italy): Possible influence of climate and fault activity: Global and Planetary Change, v. 63, p. 299-308, doi: 10.1016/j.gloplacha.2008.06.006.

Hancock, P.L., Chalmers, R.M.L., Altunel, E., and Çakir, Z., 1999, Travitonics: using travertines in active fault studies: Journal of Structural Geology, v. 21, p. 903-916, doi: 10.1016/S0191-8141(99)00061-9.

Jettestuen, E., Jamtveit, B., Podladchikov, Y.Y., deVilliers, S., Amundsen, H.E.F., and Meakin, P., 2006, Growth and characterization of complex mineral surfaces: Earth and Planetary Science Letters, v. 249, p. 108-118, doi: 10.1016/j.epsl.2006.06.045.

Leroy, J.L., Hubé, D., and Marcoux, E., October 2000, EPISODIC DEPOSITION OF Mn MINERALS IN COCKADE BRECCIA STRUCTURES IN THREE LOW-SULFIDATION EPITHERMAL DEPOSITS: A MINERAL STRATIGRAPHY AND FLUID-INCLUSION

APPROACH: The Canadian Mineralogist, v. 38, p. 1125-1136, doi: 10.2113/gscanmin.38.5.1125.

Minissale, A., Kerrick, D.M., Magro, G., Murrell, M.T., Paladini, M., Rihs, S., Sturchio, N.C., Tassi, F., and Vaselli, O., 2002, Geochemistry of Quaternary travertines in the region north of Rome (Italy): structural, hydrologic and paleoclimatic implications: Earth and Planetary Science Letters, v. 203, p. 709-728, doi: 10.1016/S0012-821X(02)00875-0.

Mort, K., and Woodcock, N.H., 2008, Quantifying fault breccia geometry: Dent Fault, NW England: Journal of Structural Geology, v. 30, p. 701-709, doi: 10.1016/j.jsg.2008.02.005.

Shipton, Z.K., Evans, J.P., Kirschner, D., Kolesar, P.T., Williams, A.P., and Heath, J., 2004, Analysis of CO2 leakage through 'low-permeability' faults from natural reservoirs in the Colorado Plateau, east-central Utah: Geological Society, London, Special Publications, v. 233, p. 43-58, doi: 10.1144/GSL.SP.2004.233.01.05.

Uysal, I.T., Feng, Y., Zhao, J., Altunel, E., Weatherley, D., Karabacak, V., Cengiz, O., Golding, S.D., Lawrence, M.G., and Collerson, K.D., 2007, U-series dating and geochemical tracing of late Quaternary travertine in co-seismic fissures: Earth and Planetary Science Letters, v. 257, p. 450-462, doi: 10.1016/j.epsl.2007.03.004.

Uysal, I.T., Feng, Y., Zhao, J., Bolhar, R., Işik, V., Baublys, K.A., Yago, A., and Golding, S.D., 2011, Seismic cycles recorded in late Quaternary calcite veins: Geochronological, geochemical and microstructural evidence: Earth and Planetary Science Letters, v. 303, p. 84-96, doi: 10.1016/j.epsl.2010.12.039.

U-zysal, I.T., Feng, Y., Zhao, J., Isik, V., Nuriel, P., and Golding, S.D., 2009, Hydrothermal CO2 degassing in seismically active zones during the late Quaternary: Chemical Geology, v. 265, p. 442-454, doi: 10.1016/j.chemgeo.2009.05.011.

WOODCOCK, N.H., and MORT, K., 2008, Classification of fault breccias and related fault rocks: Geological Magazine, v. 145, p. 435-440, doi: 10.1017/S0016756808004883.

Woodcock, N.H., Omma, J.E., and Dickson, J.A.D., 2006, Chaotic breccia along the Dent Fault, NW England: implosion or collapse of a fault void? Journal of the Geological Society, v. 163, p. 431-446, doi: 10.1144/0016-764905-067.

WRIGHT, V., WOODCOCK, N.H., and DICKSON, J.A.D., 2009, Fissure fills along faults: Variscan examples from Gower, South Wales: Geological Magazine, v. 146, p. 890-902, doi: 10.1017/S001675680999001X.

ZENTMYER, R., MYROW, P.M., and NEWELL, D.L., 2008, Travertine deposits from along the South Tibetan Fault System near Nyalam, Tibet: Geological Magazine, v. 145, p. 753-765, doi: 10.1017/S0016756808005323.

BROGI, A., CAPEZZUOLI, E., AQUE', R., BRANCA, M. and VOLTAGGIO, M., 2010, Studying travertines for neotectonics investigations: Middle to Late Pleistocene syn-tectonic travertine deposition at Serre di Rapolano (Northern Apennines, Italy): International Journal of Earth Sciences, v. 99, p.1383–1398, doi: 10.1007/s00531-009-0456-y.

Brogi A. and Capezzuoli E., Travertine deposition and faulting: the fault-related travertine fissure-ridge at Terme di S.Giovanni, Rapolano Terme (Italy): Int. J. Earth Sci. (Geol Rundsch), v.98, p. 931–948, doi: 10.1007/s00531-007-0290-z.

Çakir Z., 1999, Along-strike discontinuity of active normal faults and its influence on quaternary travertine deposition; examples from western Turkey: Turkish Journal of Earth Science, v.8, pp. 67–80.

Fong, A. W., 1995, Geologic map of the Fountain Green South quadrangle, Sanpete and Juab counties, Utah, scale 1:24 000, 2 sheets.

Lawton, T. F., and Weiss, M. P., 1999, Geologic map of the Wales quadrangle, Sanpete County, Utah, scale 1:24 000, 2 sheets.

Mesci, B. L., Gursoy, H., and Tartar, O., 2008. The Evolution of Travertine Masses in the Sivas Area (Central Turkey) and Their Relationships to Active Tectonics: *Turkish Journal of Earth Sciences*, v. 17, p. 219-240.

Ortner, H., 2003, Cementation and tectonics in the Inneralpine Molasse of the Lower Inn Valley: Geol. Paläont. Mitt. Innsbruck, v.26, p. 71–89.

Pentecost A., 2005,Travertine, Springer, Berlin , p.445.

Rowland, S. M., 2007, Duebendorfer, E. M., Schiefelbein, I. M. Structural analysis and synthesis: A laboratory course in structural geology, third edition, Blackwell Publishing Inc., Malden, p. 301.

Figure:

Basin and range province: http://rst.gsfc.nasa.gov/Sect6/Sect6_8.html

- Primary Author: Nicholas M. Short, Sr.-